# Simulation and Full-Scale Emulation of a Powertrain for Small Electric Vehicle

By

Pablo García Fuente

Submitted to the Department of Electrical Engineering, Electronics, Computers and Systems
In partial fulfillment of the requirements for the degree of
Master in Electrical Energy Conversion and Power Systems
at the
UNIVERSIDAD DE OVIEDO
July 2016



Author…………………………………………………………………………......

Pablo García Fuente
Electrical Engineer
EPI Gijón - España

Certified by……………..……………………………………………………………....

Professor Coordenador Paulo Pereirinha
ISEC – Inst. Polytech. de Coimbra – Portugal
Professor Jorge García García
EPI Gijón – España

# Simulation and Full-Scale Emulation of a Powertrain for Small Electric Vehicle

By

Pablo García Fuente

Submitted to the Department of Electrical Engineering, Electronics, Computers and Systems

On July 22th, 2016, in partial fulfillment of the requirements for the degree of Master of Science in Electrical Energy Conversion and Power Systems

## Abstract

Electric mobility is a reality that together with the purpose of “Zero $CO_2$ emissions”, optimal quality of life for the metropolis that we are building will be achieved in close future.

In this master thesis the work done on a test bench for a basic electric vehicle emulation is described. The work has started with theoretical study of the test bench in order to understand the implementation done in ISEC-IPC. Work has continued on studying and verifying of the technical infrastructure for the test bench like the traction electric motor, servomotor, and respective controllers, as well as, the Li-Ion battery system, the communication and control of the test bench with dSPACE that was setup and tuned.

When the knowledge was acquired, the implementation was changed in order to track the test bench with a basic electric vehicle which is in VEIL project. It can be tested the different modules of the test bench and test electric traction motor.

Thesis Supervisor: Paulo Pereirinha
Title: Professor Coordenador

Professor Jorge García García
EPI Gijón – España

# Acknowledgements

I am so thankful to my girlfriend, my family, coworkers and companies who made this possible. Coimbra experience was amazing both as personal as professional and I am grateful for the excellent quality service I received from ISEC in general and from scientific committee in particular.

I carry with me the famous Coimbra’s Saudade.

Pablo García Fuente

# Table of Contents

# List of Figures

# List of Tables

# Chapter One

# 1 Introduction

## 1.1 Background

Driving experiences are changing to automatic driving with autonomous car so that people will not drive anymore. When the driving assistance arrives, the activities begin to die and when usual activities begin to disappear, they are gone forever, so the essence of driving is extinguished. As an experienced driver, the author helps to contribute ideas in order to improve power train performances.

This master thesis tried to understand, check and use a test bench existing at IPC-ISEC (Institute Polytechnic Coimbra - Institute Superior Engineering of Coimbra) with a permanent magnet motor to get optimal performances of the power train in order to install, in consequence, into a small electrical vehicle, next research stage. The different analysis, studies, implementations and writing were done between 28$^{th}$ March and 22$^{th}$ July.

This proposal is also linked to an earlier funded Multiple Energy Storage systems Management Optimization for Electric Vehicles project (MESMO-EV), where the test bench was implemented using NI-LabVIEW as software and Compact-RIO and dSPACE as platforms. In this case, this test bench is to use dSPACE interface and Simulink models.

## 1.2 Objectives

The central theme of the thesis is based on checking the methodology implemented in MESMO-EV project and evaluate developments in secondary tech bench done. This can help to prepare new project proposals or to implement the future setup in a small electric vehicle. The fundamental objectives guiding the work process can thus be listed to:

- Understand all the components of the tech bench, check its implemented and verify if its working.
- Development of powertrain test bench for the small electric vehicle based on dSPACE and HIL Matlab/Simulink models which was developed for similar EV using another experimental implementation.
- Simulation/emulation of the small EV behavior for test driving cycles.

## 1.3 Thesis Structure

Towards the previously mentioned objectives, the thesis work was developed, and the structure is organized as follows:

**Chapter 1: Introduction**

This present chapter introduces the motivation for the work carried out in this thesis.

**Chapter 2: Literature Review**

This chapter reviews the research literature for the work carried out in this thesis.

**Chapter 3: Hardware Setup Detail**

This chapter and the next ones describe the work methodology: equipment, technologies and theories applied during the thesis. The main equipment are:

- ✓ $LiFePO_4$ Sinopoly Batteries: SP-LFP40AHA.
- ✓ Lithium battery charger: GWL-Power-POW72V35A.
- ✓ Battery Management System: BMS123 Main controller.
- ✓ SEVCON Synchronous Motor Controller: Gen4-72-80VDC.
- ✓ Permanent Magnet Synchronous Motor (PMSM): Heinzmann GmbH PMS120.
- ✓ Variable Frequency Drive (VFD): SEW-EURODRIVE: MDX60a022050J-4-00.
- ✓ Permanent Magnet Synchronous Motor (Servomotor): SEW-EURODRIVE. Model: CMP80M/KY/RH1M/SM1.
- ✓ dSPACE MicroAutoBox II 1401/1511-1512.

**Chapter 4: Implementation**

This chapter includes the procedures performed during thesis.

- ➢ Analyze MESMO-EV project: study some of the most relevant publications, check implementations and developments related with second test bench.
- ➢ Analyze batteries behavior. Analyze battery management system and establish a safety protocol to charge the battery pack through Lithium battery charger. Analyze behavior of the battery pack in discharge stage. (Behavior while battery pack is discharging).
- ➢ Analyze SEVCON performance, connections between batteries and PMSM.
- ➢ Test the experimental setup for battery pack, SEVCON and PMSM mechanically.
- ➢ Analyze PMSM and VFD performances, connections and communications.

- Test the experimental setup for SEW and EURODRIVE mechanically.
- Analyze dSPACE performances, connections and communications.
- Design implementation in Simulink to dSPACE in order to control both systems.
- Verification of the built prototype.

**Chapter 5: Conclusions and Outlook**

This chapter indicates the conclusions reached out of the thesis work and outlooks a future path for research in this field. For this thesis, theoretical requirements are fulfilled successfully, so this implementation can be installed in electric vehicle or to be used in future project proposals.

# Chapter Two

# 2 Literature Review

## 2.1 Global terms

The idea began in 1988 in the "Toronto Conference on the Changing Atmosphere" in Canada. Since then there were several other conferences on the environment and climate where was discussed and negotiated the creation of the Kyoto Protocol, Japan, in 1997.

In 1990, the Intergovernmental Panel on Climate Change was created in order to alert the public about global warming. In 1992, it was the turn of the Eco'92 where it was decided that the countries were responsible for the conservation of climate regardless of the size of the nation in question. The protocol entered into force in 2005 and showed the interest of countries to use carbon as currency.

China is the first country issuing the world's carbon. The US, like second country issuing the world's carbon, refused to ratify the protocol on the grounds that to accept it would be bad for the US economy. The unwillingness of the richest and most polluting countries is a major impediment for something to be done effectively against global warming. In 2012 the Protocol had their validity extended until 2020 after the Conference of the Paris (COP18) and some countries published strict target for next years.

For other hand, every four years there is the United Nations Climate Change Conference (UNFCCC) in order to closely monitor the situation in the near future, to make sure this environmental protocol in implemented.

This environmental protocol has forced to change the development model of the world powers, and instead, have benefitted developing country, placing them like example to follow.

As far as our own area of responsibility is concerned, electrical energy that feed the world needs a radical change of minds. $CO_2$ emissions, losses and dependency are main factors to decrease.

The investment in renewable energies and smart grids and electric mobility are the key as solution.

If demand energy is divided in four big groups: buildings, industry, transport and electricity; the investment shall be set at the following levels:

- Buildings: Optimize consumption with efficient equipment and suitable insulation. Including renewables energies and applying an energetic certificate for new buildings and commercial places, it is possible to obtain better performances.
- Industry: Optimization of the manufacturing process. Update technology for intensive production. Include Energy Regenerated in industrial processes.
- Electricity: More energy generated with 0 % $CO_2$ emissions (Renewable energy sources). Measures installation to decrease $CO_2$ levels in conventional power sources. Researching and updating transmission electrical networks in order to improve efficiency.
- Transport: For population, this point takes more importance than building because it is suffered each day. The high density of vehicles in the world's cities produces directly pollution over population. It is combined with “petrol show” in disorder prices, business, politics, and wars; and reproduced in all social-media like internet, TV, newspaper, radio.

After this perspective, to avoid destroying the world and to develop electric vehicles, researchers and engineers have been working hard to solve several issues concerning the technology involved and creating possible alternatives.

This technological revolution in the transport can be separated in three fields: vehicles, bio energy and hydrogen & full cells.

In the first field, the advances in engine efficiency and lightweight materials have produced a remarkable evolution in conventional vehicles. However, they are not a clean and efficient alternative (efficiency around 20-30 %). An alternative implemented in some countries is to replace non-renewable source of energy (petrol-diesel) for another non-renewable source of energy, in this case, gas. This might produce increased profitability due to GLP price is up to 10 times less than petrol (Portugal: 1.53 €/l petrol vs 0.45 €/l GLP), but the energetic efficiency is smaller.

As alternative for conventional combustion engine, electrical vehicles have grown up progressively, its well-to-wheel efficiency using renewable energy sources, can get up to 65 %. However they still have important challenges with the batteries. At the next chapter is explained insightfully. In addition, there is a combination of drive train technologies, the so called hybrid system which consists on using an internal combustion engine plus an electric motor. This system is used in several types of vehicles: Rail transport, cranes, military off-road vehicles, ships, aircrafts and commercial & road transport vehicles. Last alternative is hydrogen & full cells; a fuel cell uses the chemical energy of hydrogen or another fuel to cleanly and efficiently produce electricity. If hydrogen and oxygen are the fuel, then electricity, water, and heat are the only resulting products. It is an experimental technology in vehicles, in others terms, which will be much spoken of in the future.

Today, each manufacturer has invested in his appropriate technology looking for an alternative to internal combustion engine.

In this second field, bio energy researchers and scientist have been working to develop renewable biofuel in order to substitute for crude oil, gasoline, diesel fuel, and jet fuel. In addition, the conversion to crude oil to different fuels and theirs qualities has been improved during these years. An example of this would be the Efficiency Energy & Renewable Energy Office (EERE) [1] from US that is researching about following areas:

- Processing and Conversion: Developing technologies that can efficiently convert feedstocks into transportation fuels, bio-products, and bio-power.
- Algal Biofuels: Breaking down technical barriers and promoting sustainable, affordable, and scalable algae-based biofuels.
- Bio-refinery Projects: Funding bio-refinery projects from the pilot, demonstration, and commercial scales.
- Analysis: Applying analytical tools, data, and methodologies to identify research and development pathways that offer the greatest potential for commercialization
- Feedstock Supply: Identifying and developing efficient, sustainable, renewable, biological materials for the production of clean energy.
- Sustainability: Ensuring that efforts to develop bioenergy do not compromise environmental quality or the availability of food, feed, fiber, and water.
- Feedstock Logistics: Designing and developing advanced equipment and systems to reduce cost, improve biomass quality, and increase productivity throughout the biomass logistics chain.
- Bio-power: Enabling increased use of biomass to generate electricity, heat, and power.

In the third field, hydrogen is the simplest element on earth—it consists of only one proton and one electron—and it is an energy carrier, not an energy source. Hydrogen can store and deliver usable energy, but it does not typically exist by itself in nature and must be produced from compounds that contain it. Hydrogen can be used in fuel cells to generate power using a chemical reaction rather than combustion, producing only water and heat as byproducts.

Fuel cells are unique in terms of the variety of their potential applications; they can provide power for systems as large as a utility power station and as small as a laptop computer [1]. It is a booming research field due to if the production, distribution and use of hydrogen is achieved, it would be the best alternative for the world.

In the production of hydrogen main work is in the following areas:

- Biomass-derived liquid reforming.
- Electrolysis.
- Biomass Gasification.
- Thermochemical water splitting.
- Photo-electrochemical water splitting.
- Photo-biological Processes.
- Microbial biomass conversion.

## 2.2 Electric vehicle

The electric vehicle has always been the neglected child. Although its first developments occur at the same time as internal combustion vehicles, it has always been kept in the drawer of oblivion by the empire of crude oil.

The sustainable mobility paradigm has been proposed in response to concerns of the wide ranging negative outputs of current mobility systems, including climate change, social exclusion, resource consumption and air pollution. It calls for "a radical change in the way in which travel decisions are made". The approach is developed around three needs as first, to reduce the need to travel and consequently lead to less trips; as second, to encourage modal shift towards more sustainable options, and as third, reduce the length of trips. Two approaches to achieving more sustainable mobility could arguably be through technological innovation such as Electric Vehicles (EVs) and behavior changes leading to increased energy efficiency [2].

Volkswagen Group VW AG, made a study about population mobility where they got awesome results. 78 % of population reached less 50 km per day. 19 % population reached less 150 km per day and only 3 % reached upper 150 km [3].

Therefore, electric mobility is a real and zero-emissions solution and complies with daily routine. What is the problem? Close mind, also global crisis, people are living day to day. They cannot focus on a long-term view because the electric car requires a high initial payment. If the technical problems to improve are checked, it is necessary to divide by parts to analyze separately.

### 2.2.1 Batteries

Batteries are the crucial component in electric vehicles. It relates aerodynamic, autonomy behavior with his heavier burden and capacity. This piece breaks the high efficiency from electric cars (60-70 %). It is necessary to make an electrical study from materials for battery pack. The differences between various batteries are shown in Table 2.2.1.

Table 2.2.1 Comparison of battery classical chemistries [4].

| CATHODE | LI-ION | PB-ACID | NI-CD | NI-MH |
|---|---|---|---|---|
| Lifetime / cycle | 500~1000 | 200~500 | 500 | 500 |
| Working potential / V | 3.60 | 1.00 | 1.20 | 1.20 |
| Specific energy / Wh $kg^{-1}$ | 100 | 30 | 60 | 70 |
| Energy Density / Wh $L^{-1}$ | 240 | 100 | 155 | 190 |

Table 2.2.2 Electrochemical parameters of several cathode materials [4].

| CATHODE | $LiFePO_4$ | $LiFePO_4$ +5%C | $LiMn_2O_4$ | $LiCoO_2$ | $LiNi_{0.8}Co_{0.2}O_2$ |
|---|---|---|---|---|---|
| Density / g $cm^3$ | 3.60 | 3.48 | 4.31 | 5.10 | 4.85 |
| Potential / V | 3.50 | 3.50 | 4.05 | 3.90 | 3.60 |
| Specific capacity / mAh $g^{-1}$ | 169 | 159 | 148 | 274 | 274 |
| Specific energy/Wh $g^{-1}$ | 0.59 | 0.56 | 0.56 | 0.98 | 0.98 |

$LiCoO_2$ was first chosen to work as cathode materials when Li-ion batteries come out in 1990. Its long history supports $LiCoO_2$ a big progress. During that process, other cathode materials were discovered: $LiNiO_2$, $LiMn_2O_4$, $LiNi1/3Co1/3Mn1/3O_2$, $LiFePO_4$, and others. Comparisons of electrochemical parameters of several cathode materials are listed in
Table 2.2.2.

$LiFePO_4$ is currently under extensive studies due to its low cost, low toxicity, high thermal stability and high specific capacity of 170 mAhg−1. Reduced reactivity with electrolytes results in the very flat potentials during charge-discharge processes. The most prominent advantages of $LiFePO_4$ are that the structure of material hardly changes with Li ion intercalation and deintercalation and it holds a long voltage platform.

#### 2.2.2 Electric Motors

It can be said that the majority of the motors being used in electric cars are the 3 phase AC motor, the series wound DC motor and the permanent magnet motor. The comparison should be done from balancing factors what people wants for them. At first point cost, The DC motors usually cost less than AC motors, DC motors are often easier to find locally than AC motors. For terms of size, powertrain behavior, efficiency and requirements, it was chosen a permanent magnet motor.

#### 2.2.3 Technologies

At this stage, the connection through the motor controller between the battery system and the permanents magnet motor is explained. Technology that is able to manage the flow of energy demanded by the motor in real time is required.

Each controller manufacturer offers custom software with his product, producing a certain number of software without communication between them. There are specific technologies that allow communication and management of motor, controller, batteries, taking into account road demand. The test-bench has a servomotor to impose the drive efforts which implies another controller and software. The possibilities of the market offers are three alternatives as hardware controllers: CompactRIO, dSPACE, Opal RT.

## 2.3 Conclusion

In this chapter, it was reviewed the environmental global situation during these years and the evolution in automotive area. It can be seen as technological revolution is real. Climate change, the global crisis and the high levels of pollution in cities, have sensitized governments to act collectively to a problem that affects everyone. Both public and private research have led to the deployment and search of the ultimate technology to solve the riddle of energy storage and distribution to the world's population with efficiency and cleaness. Now, we are seeing how countries are restricting conventional energies and industries, forcing raise awareness of the change in a few years.

For automotive area, the evolution is progressive; manufacturers are working hard to comply with strict rules from environmental commissions. The ultimate power source for them is unknown yet. Lithium has limitations but alternatives like hydrogen & fuel cells are still far away.

In this thesis terms, it can be seen that $LiFePO_4$ are a good battery solution for EV today. As similarly, permanent magnet synchronous motors for EV traction are a very interesting option.

Regarding possible hardware control platform for the test bench, CompactRIO does not have the desirable processing capacity to deal with the project. Also only works with NI LabVIEW which implies to convert Matlab/Simulink models to LabVIEW. Concerning dSPACE, it has a good processing capacity and it can support more complex algorithms, for example, for optimization.

It’s a modular technology, so it can be decided which parts to buy. One advantage from CompactRIO is high number to I/O in analogue, digital and communication. About the price, quality-price depends on modules needed it. It works with Simulink tool.

OPAL RT has good performances as dSPACE, supports different algorithms within take into account size and processing capacity. The quality is higher than others however its more expensive.

# Chapter Three

# 3 Hardware Setup Detail

This work is also linked to the earlier MESMO-EV project, where it was implemented a similar test bench using NI LabVIEW as software and Compact-RIO as platform. In this case, this test bench uses dSPACE interface and Simulink models. Below, the main components are shown for each level.

In this chapter, a short description of the main equipment of the test bench is done using mainly the most relevant information extracted from the manufacturer technical documentation.

## 3.1 Power supply

Test bench power supply consists in 80 Vdc output with a battery system and battery management system (BMS) that maintains all batteries balanced as unique battery.

### 3.1.1 Batteries

The battery system is formed by 24 x 2 cells in parallel giving 80 Vdc like nominal output. It is an industrial lithium cell with high energy density, made on the safe $LiFePO_4$ technology from a specialized manufacturer Sinopoly [4]. The technical data is the following:

- Manufacturer: Sinopoly.
- Model: SP-LFP40AHA.
- Nominal Voltage: 3.2 V.
- Voltage range: 2.8 ~ 3.65 V.
- Maximum charging voltage for initial charge: 3.7 V.
- Recommended subsequent charging: 3.65 V.
- Minimum voltage: 2.65 V.
- Optimal discharge current: 13 A
- Maximum discharge current: 120 A in 3C continuously.
- Maximum charging current: 8 A.
- Operating temperature charging: 0 ~ 45 ºC
- Operating temperature discharging: -20 ~ 55 ºC.
- Weight: 1.5 kg.

These battery cells are suitable for all traction applications including passenger cars. Fully complies also for stationary applications such as energy storage. They can be recharged at any state of discharge. There is no significant memory effect; $LiFePO_4$ is a very safe technology, not spontaneous combustion, does not react with moisture or with oxygen. Manufacture's specifications are showing in the following Figure 3.1-1 and discharge curves in Figure 3.1-2.

Figure 3.1-1 SP-LFP40AHA specifications [5].

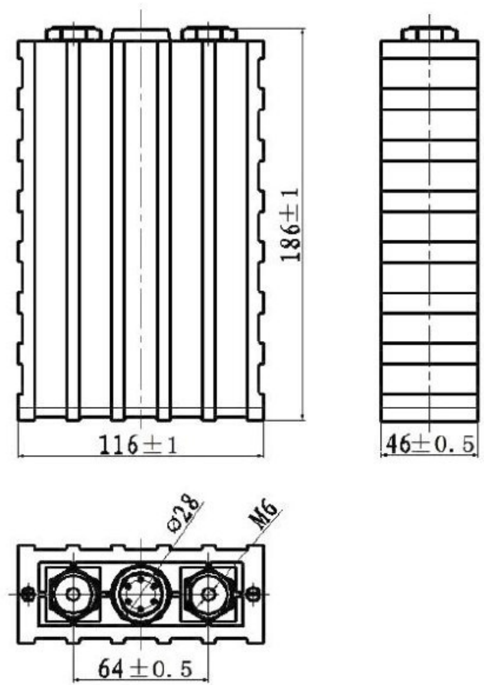

Figure 3.1-2 SP-LFP40AHA discharge cure under normal temperature [5].

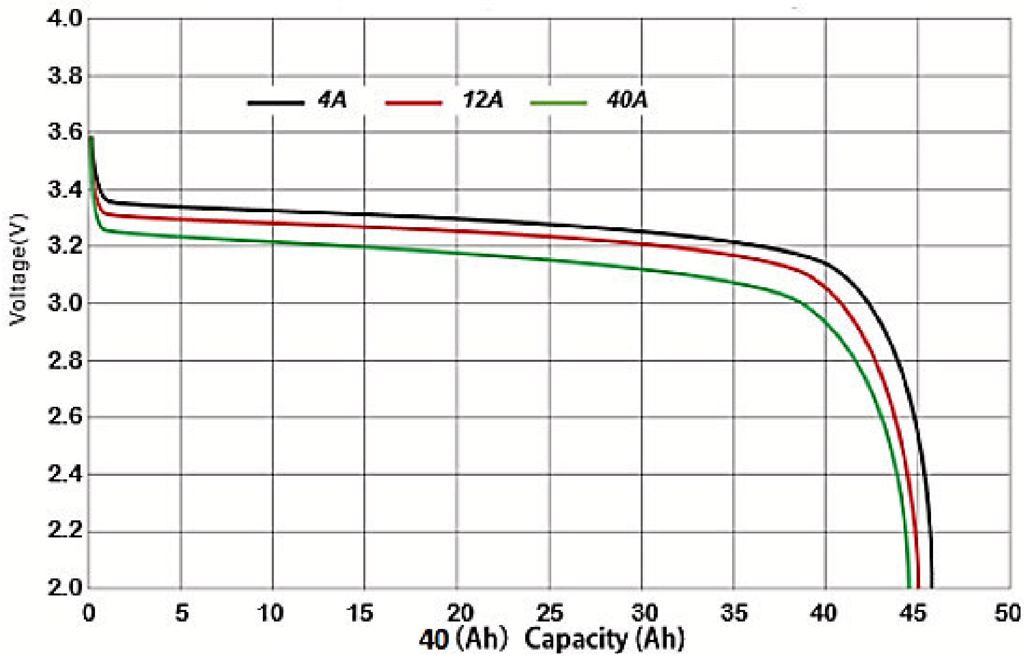


### 3.1.2 Charger

Taking into account the batteries manufacturer, it is advisable to choose the charger thinking also on the battery management system because some chargers have incorporated management system connection. For this case, POW72V35A/BMS from GWL/Power facilities comply with our requirements and battery management system connection [5]. The main technical characteristics are the following:

A. Input characteristics:
   - Manufacturer: GWL/Power Group Technology Solutions.
   - Model: POW72V35A/BMS.
   - Rated input voltage: 230 Vac.
   - Input voltage range: 180 ~ 264 Vac.
   - AC input voltage frequency: 47 ~ 63 Hz.
   - Maximum input current: 16 A.
B. Output characteristics:
   - Nominal charge voltage: 72 Vdc.
   - Fast charge voltage: 88 Vdc.
   - Maintain voltage: 88 Vdc.
   - Constant current: 35 A.
   - Deep Voltage level: 65 Vac.
   - Deep discharge current: 3 A.
   - Power efficiency: > 80 %.

This product also has connection to battery management system which allows the charger to work with different charge currents. The charging curve can be showed in Figure 3.1-3.

Figure 3.1-3 POW72V35A/BMS charging curve (current A-red, voltage V-blue) [6].

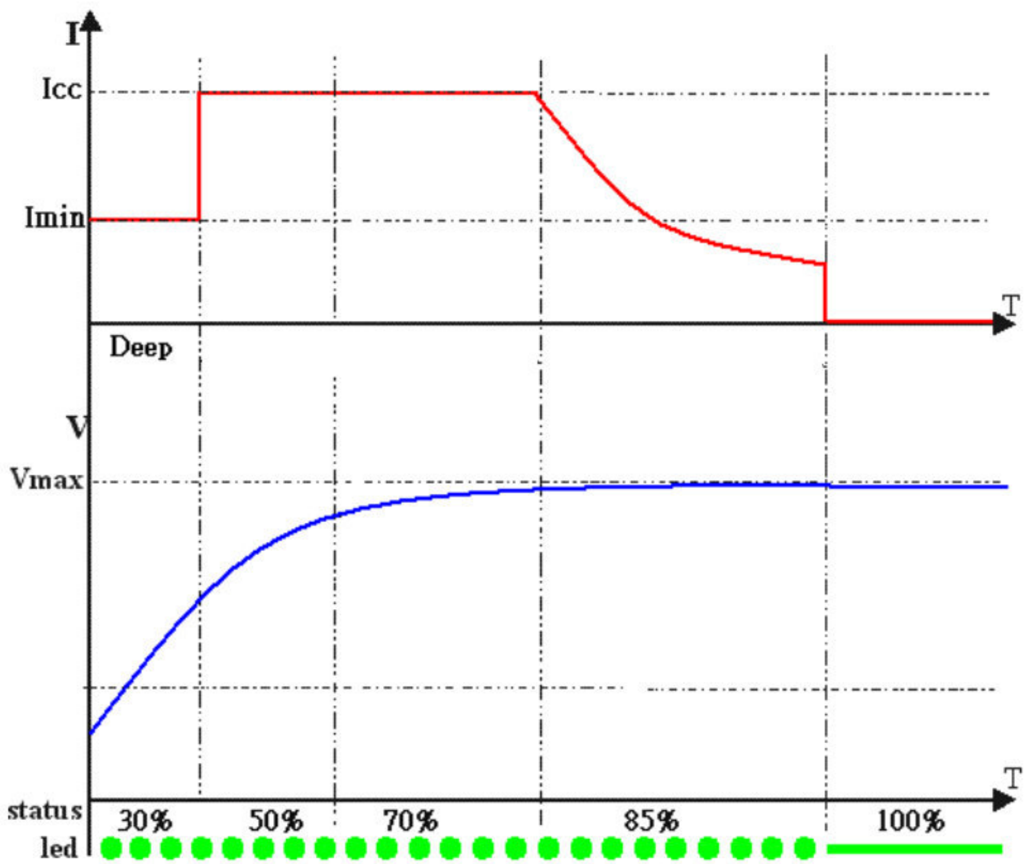


### 3.1.3 Battery Management System

The BMS, is primarily intended for prismatic $LiFePO_4$-cells, but can also be adapted for other cells like Li-Ion and LiPo, provided that the cell-voltage is in the range of 2 V to 5 V.

The BMS is designed for battery-packs that have many cells in series/parallel, to form a high voltage battery-pack. Each cell is equipped with a small BMS-board that monitors cell parameters like cell-number, cell-voltage, cell-temperature and bypass-current. These boards send this data via a one-wire interface to the BMS-controller. This controller collects all this data, and displays that via a USB-interface on a Windows Computer.

For the implementation it was decided to make a circuit of 24 series parallel placing 2 cells in parallel in each series. The number of BMS cell boards is reduced by half and each BMS-board measures the voltage across the parallel of cells.

To get a perfect operating life for the batteries, it is necessary to configure a safe area to work. BMS pre-sets the Coulomb counter to 100 % when either all cells get to V-bypass or when one cell reaches V-max. As it can be seen in Figure 3.1-4, the green area is the safe area where it is recommended to operate. So, in BMS software should be configuring it.

Figure 3.1-4 BMS operating curve [7].

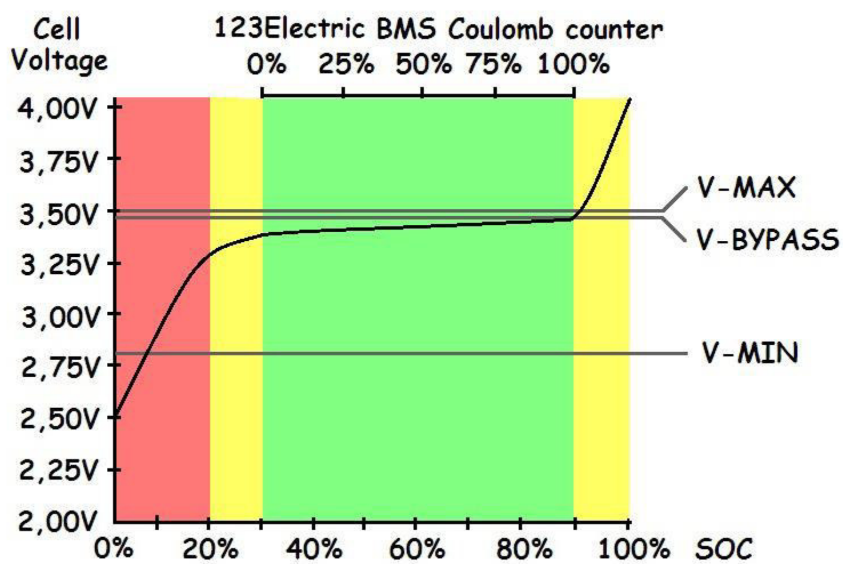


For these technical settings, it is necessary to take into account the BMS specifications [6]:

- Supply Voltage: 8-30 Vdc.
- Idle current (inclusive current sensor): < 0.007 A.
- Number of cells: 2 - 255.
- Balancing current: 1 A.
- Idle-current BMS-board: 1 A.
- Current sensor: 100/200 or 400 A.
- A/D resolution 1024 steps (10 bits).
- Cell voltage: 0.01 V steps (2 - 5 V).
- Cell temperature: 1 ºC steps (- 40 ~ 99 ºC).
- Scan time per cell: 0.015 s.
- Factory settings:
  - Vmin/Vmax/Vbyp/Vchg: 2.50 / 3.75 / 3.40 / 3.00 V.
  - Tmin/Tmax: + 0 ~ 60 ºC.

The charging algorithm considered is balanced charge. When one of the cells reaches the minimum voltage, the charging-process begins. The current slowly increases to the maximum charging current selected until one of the cells reaches the bypass-voltage. At that point the charging current will ultimately be reduced to the minimum charging current selected. Charging ends when one of the cells reaches the maximum cell voltage or when all cell reach the bypass voltage.

The battery bank was previously built but some details will be given the wiring diagram used by the BMS like shows Figure 3.1-5. It is a required remark that our design has 2 parallel in each series. In addition, it shows the mounting assembly forming the power system of our test bench. The most important here is follow a safe and clean working in assembly stages to ensure the success (Figure 3.1-6).

After mounting, after first experimental test and first charging, it is necessary to install electrical safety precautions due to other people is working in the laboratory, cleaning staff and yourself for the next stage.

In this case, the security measures taken are the following:

- ✓ Each battery terminal has an insolation plug with polarity color.
- ✓ Each battery connector is an isolated clamp.
- ✓ An insulating surface over battery system pack to prevent material falls to lower levels, accidental contacts at different potential levels.
- ✓ The charger and BMS have a miniature circuit breaker (16-1 A respectively).
- ✓ Another insulating surface over test bench table to insulate table to prevent material falls to lower levels, accidental contacts at different potential levels.

Figure 3.1-6 shows safety protocol activated where:

A. Insulating surface over battery (provisionally wood).
B. Insulation plug with polarity color.
C. Insulated clamp.
D. Insulating surface over table (rubber).
E. Metallic table to protect.

In this master work all the wiring was verified and some terminals and wires had to be replaced in order to prevent and repair some bad electrical contacts.

**Figure 3.1-5 BMS wiring diagram.**

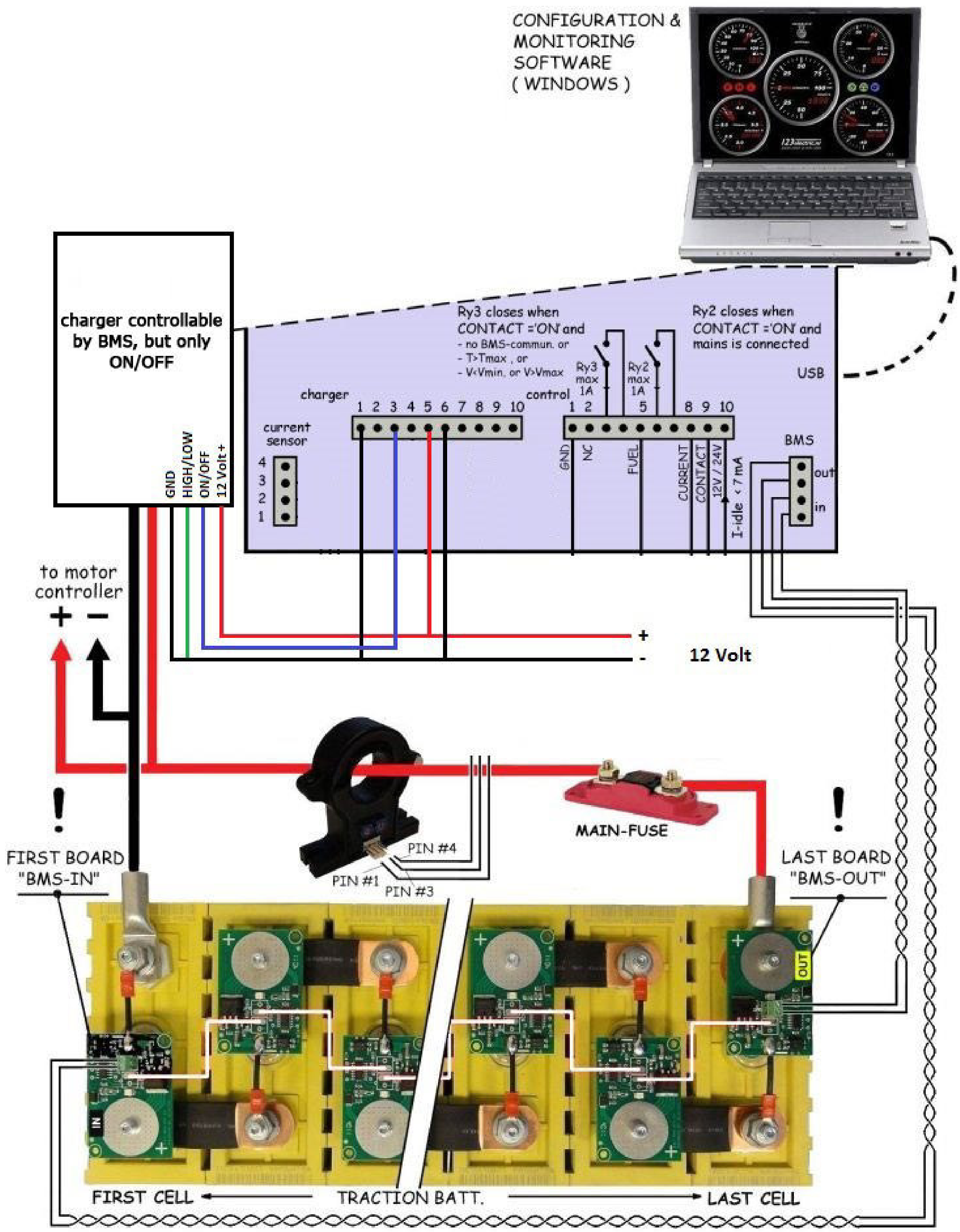

Figure 3.1-6 Safety protocol in battery system pack.

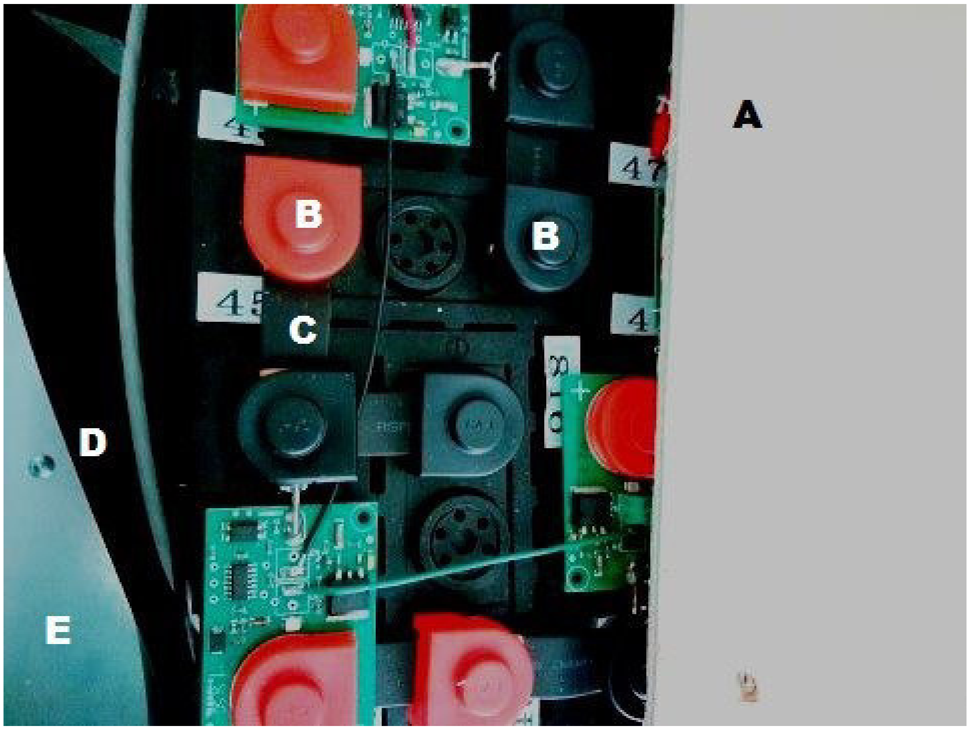


## 3.2 Electric motor

In MESMO-EV Project, it was decided to choose a permanent magnet motor for the traction motor because:

- ✓ PMSM demands low voltage for batteries.
- ✓ High torque to start up.
- ✓ Thermal properties.
- ✓ Size and volume.
- ✓ High efficiency.

Therefore, the electric motor is a permanent-field, brushless synchronous disc armature motor (axial flow motor) from HIENZMANN electric drives [7].

The specifications are the following:

- Manufacturer: HIENZMANN.
- Model: PMS 120.
- Voltage: 80 Vdc.
- Output Power: 7 kW.
- Speed: 4500 rpm.
- Torque: 14.9 Nm.
- Current: 98.5 A.
- Stall Torque: 17.8 Nm.
- Stall current: 118.2 A.
- Maximum stall torque: 45 Nm.
- Maximum stall current: 300 A.
- Back-EMF constant: 10.2 V / 1000 $min^{-1}$.
- Torque constant: 0.15Nm / A.
- Inertia: 26.3 kg / $cm^2$.
- Weight approx.: 12.3 kg.
- Degree of protection: IP54.
- Ambient Temperature: - 10 ~ 40 ºC.
- Cooling: External ventilation.

## 3.3 Motor Controller

To connect the batteries to a motor, its necessary drivers which are designed to control 3 phase motor and Permanent Magnet Synchronous Motor (PMSM) in battery powered traction and pump applications.

In a traction application control commands are made by the driver using a combination of digital controls (direction, foot switch, seat switch, etc.) and analogue controls (throttle and foot brake). The controller provides all the functions necessary to validate the driver's commands and to profile the demand for speed and torque according to stored parameters.

Throttle inputs can be configured as speed or torque demands with throttle-dependent speed limits: in either case, a torque demand is continually calculated to take account of pre-set limits on the level and rate-of-change of torque. The torque demand is used to calculate current demands; that is, the controller calculates which currents will be required within the motor to generate the required torque.

There are two distinct components of the current, known as the d-q axis currents, which control current flow in the motor. The d-axis current is responsible for producing magnetic flux, but does not by itself produce torque. The q-axis current represents the torque producing current.

Measured phase currents and current demands $i_d$ and $i_q$, the d-q axis currents, are used as part of a closed-loop control system to calculate the necessary voltage demands for each phase of the motor. Voltage demands are then turned into PWM demands for each phase using the Space Vector Modulation (SVM) technique. SVM ensures optimum use of the power semiconductors.

The motor controller for the test bench is a SEVCON Gen4 Synchronous Motor Controller [8]. The specifications are the following:

- Manufacturer: SEVCON.
- Model: GEN 4. Size 4.
- Nominal battery voltage: 80 Vdc.
- Maximum operating voltage: 116 Vdc.
- Minimum operating voltage: 19.3 Vdc.
- Peak current (2 min): 350 A.
- Boost current (10 sec): 420 A.
- Continuous current (60 min): 140 A.

The dimensions are shown in Figure 3.3-1.

For constructing and assembling motor controller, it has all the necessary mechanical and thermal equipment. It is required apply EMC protocol and thermal dissipation protocol taking into account operating process.

For connections, it is used “Connection Diagram SEVCON GEN4 – Power Supply” and “Connection Diagram SEVCON GEN4 control cabeling” from SEVCON Controller Connection Diagram V1.8 file as showing in Figure 3.3-2 and Figure 3.3-3 respectively [9].

In addition, it shows the mounting assembly forming the motor controller of our test bench. The most important here is follow a safe and clean working in assembly stages to ensure the success. It was more complicated than power supply verification due to special connector and materials.

Figure 3.3-1 Dimensions SEVCON Gen4 Synchronous Motor Controller SIZE 4 [10].

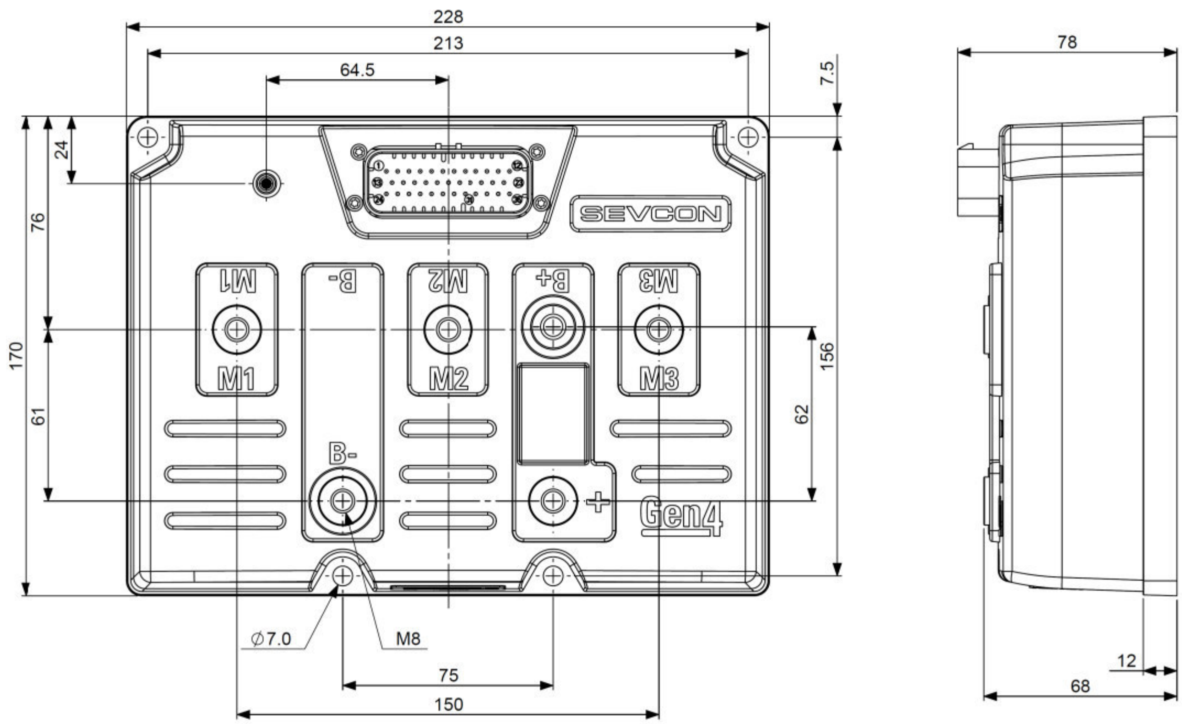


After mounting, it is necessary to install SEVCON software to turn on electrical motor. As power supply, safety precaution is applied with insulation in each connection.

This controller is protected against short-circuit to the battery positive and negative terminals. Connectivity and interoperability with other system devices using a CANbus and the CANopen protocol is provided. At first time, it is used the C6944 Shiroko Design Verification Test system (DVT), it is customer version from SEVCON. It allows the user to turn on electrical motor and measure variables through CAN [10]–[12].

After studying the electric motor and its controller, checking the wiring, the motor controller software was also studied and tested.

Here, it can be said its finished second stage of verification.

Figure 3.3-2 Connection Diagram SEVCON GEN4. Power Supply [11].

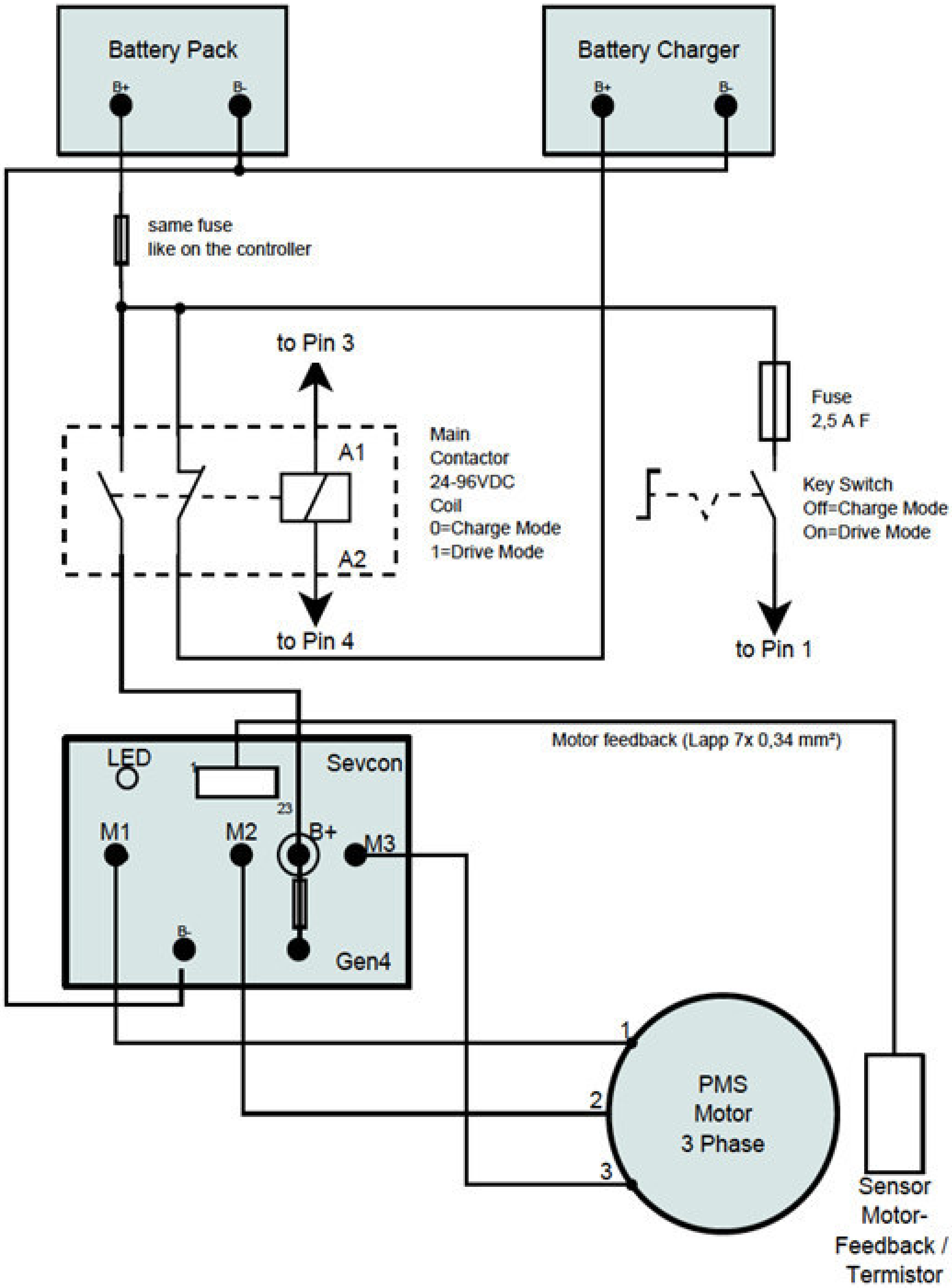

Figure 3.3-3 Connection Diagram SEVCON GEN4. Control Cabeling [11].

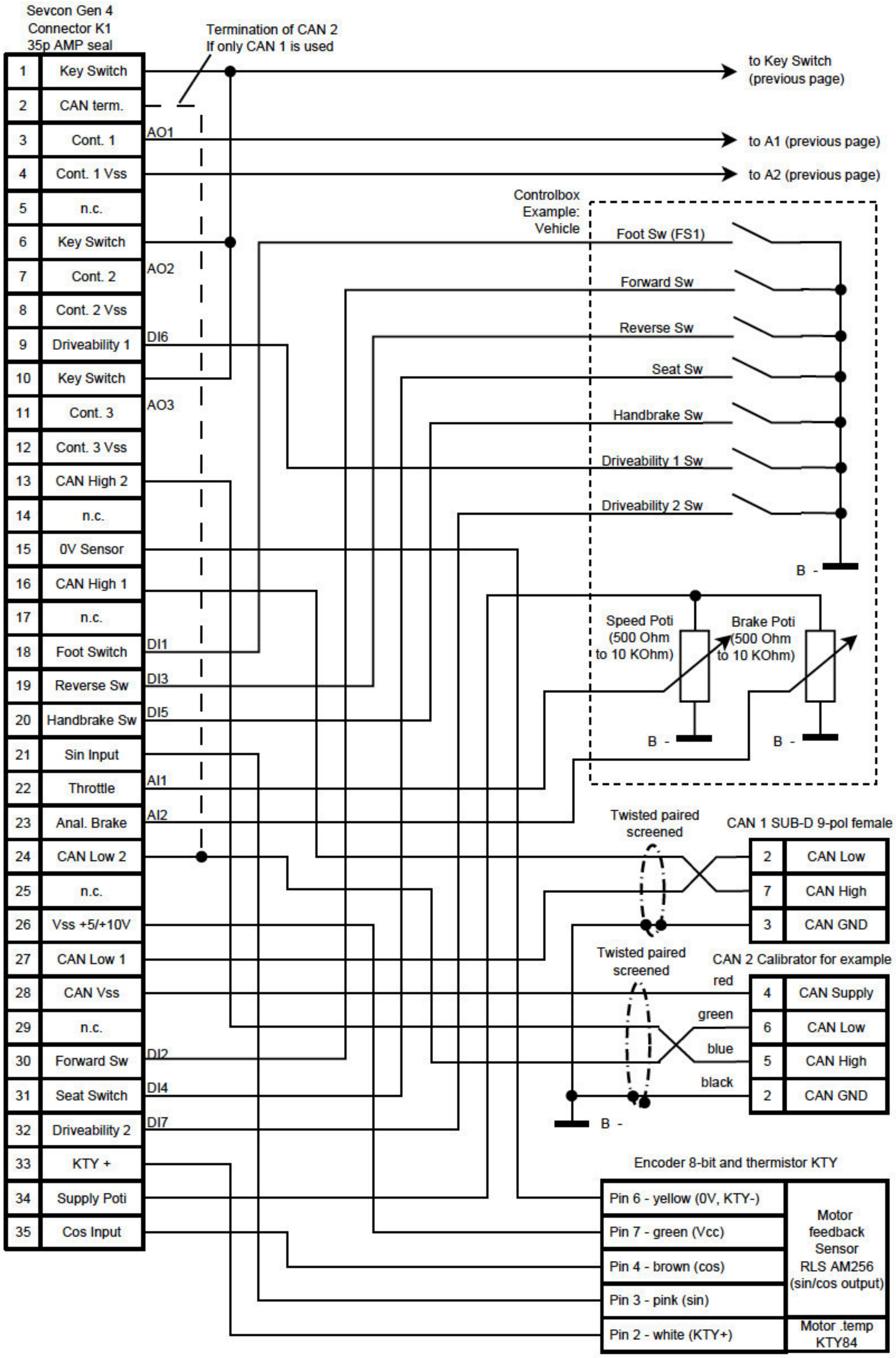

## 3.4 Servo Motor and controller

Up until now, the electric vehicle on bench prototype composition was explained however it's important to talk about another piece in this puzzle, the road. The simulation/emulation needs a system load applied to the PMSM that produce virtual road. For this case, in ISEC secondary test bench, it is used a SEW-EURODRIVE servomotor : MOVIDRIVE® MDX60/61B controlled by drive inverter, this module with servo motor complies requirements for this master thesis. Furthermore, due to collaboration agreements between SEW-EURODRIVE and ISEC, SEW supplies an assistant support and software to motor managing [13], [14].

If the model is checked, the new B series MOVIDRIVE® drive inverters are impressive devices with extensive basic functions, a wide power range, great overload capacity and a modular unit design. They facilitate unrestricted application of AC drives with 0.55 to 160kW (0.75 to 215hp) with the most modern digital inverter technology. With MOVIDRIVE®, even asynchronous AC motors can achieve levels of dynamic performance and control quality that were previously only possible using DC motors.

The integrated control and expansion options using technology and communication options create remarkably cost-effective drive systems as regards diversity of application, project planning, startup and operation. The SEW-EURODRIVE drive inverter and motor technical rating plates are described in the following list, and the specifications are show in Figure 3.4-1.

A. MOVIDRIVE® drive inverter:
   - Model: MDX60A0220-503-4-00.
   - Input Voltage: 3 ~ 400 V or 500 V.
   - Input Frequency: 50 / 60 Hz ± 5 %.
   - Input Current: 41.4 A (at 400 Vac and 100 % I).
   - Temperature: 0 ~ 40 ºC.
   - Degree of protection: IP20.
   - Output Voltage 3 ~0 V. U netz.
   - Output Frequency: 0 ~ 599 Hz.
   - Output Current: 46 A. (at 400 Vac).
   - Output Apparent Power: 31.9 kVA.

B. SERVO MOTOR.

- Model: CMP80M/KY/RH1M/SM1.
- Torque: 18.70 Nm.
- Maximum Torque: 62.60 Nm.
- Current: 20.10 A.
- Maximum Current: 103 A.
- Speed: 0 ~ 4500 rpm.
- Nominal Frequency: 375 Hz.
- IP65. IMB5.
- Voltage sys \ Peak Voltage: 400 \ 283 V.
- Weight: 15.037 kg.

Figure 3.4-1 Dimensions for MDX60A/61B size 3, dimensions in mm [15].

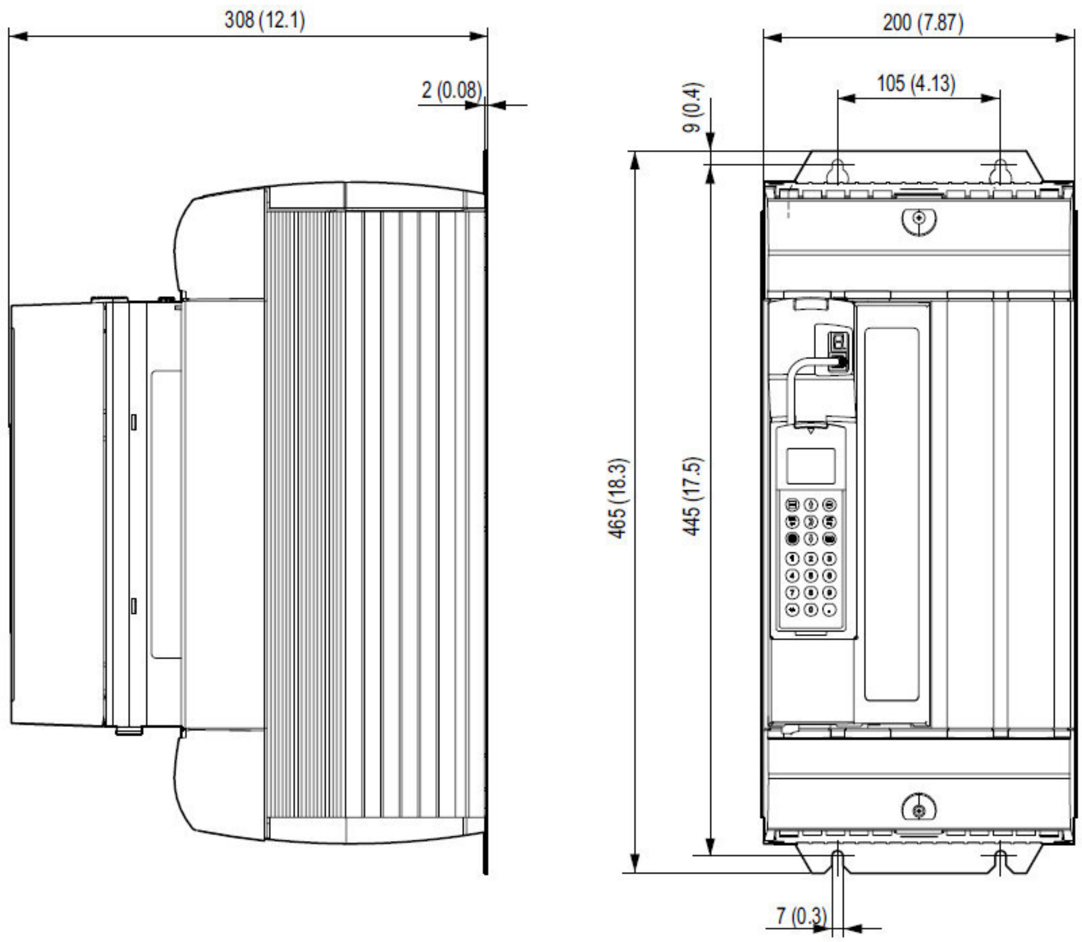

The control of MOVIDRIVE® is done through DBG60B key pad or interface adapter. DGB60B functions are the followings and the dimensions are showed in Figure 3.4-2:

- Display process values and status.
- Status displays of the binary inputs/outputs.
- Error memory and error reset queries.
- Option to display and set the operating parameters and services parameters.
- Data backup and transfer of parameters sets to other MOVIDRIVE® units.
- User-friendly startup menu for VFC mode.

Figure 3.4-2 Dimensions for MDX60A/61B size 3, dimensions in mm [15].

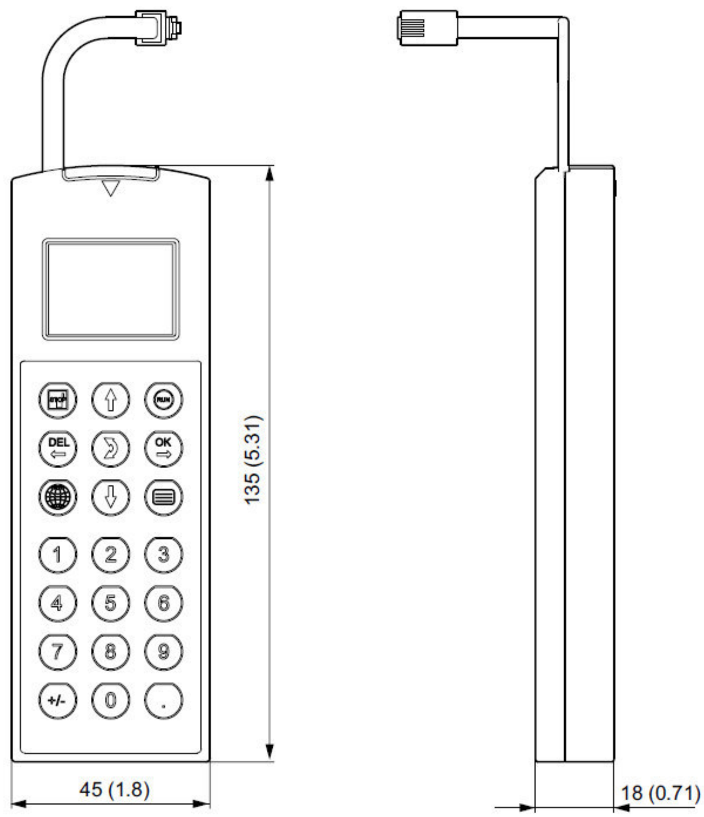


For other hand, interface adapter type USB11A enables a PC or laptop with a USB interface to be connected to the XT slot of MOVIDRIVE®B. The USB11A interface adapter supports USB 2.0 and should be connected using a serial interface cable with RJ 10 connectors.

The dimensions are showed in Figure 3.4-3 and the technical data is the following:

- Model: MOVIDRIVE®B USB11A. 824 831 1.
- Ambient temperature: 0 ~ 40 ºC.
- Storage temperature: - 25 ~ 70 ºC (according to EN60721-3-3, class 3k3).
- Degree of protection: IP20.
- Weight: 300 g.
- Dimensions: 92.5x43x25 mm.

Figure 3.4-3 Dimension drawing for DBD60B, dimensions in mm (in) [17].

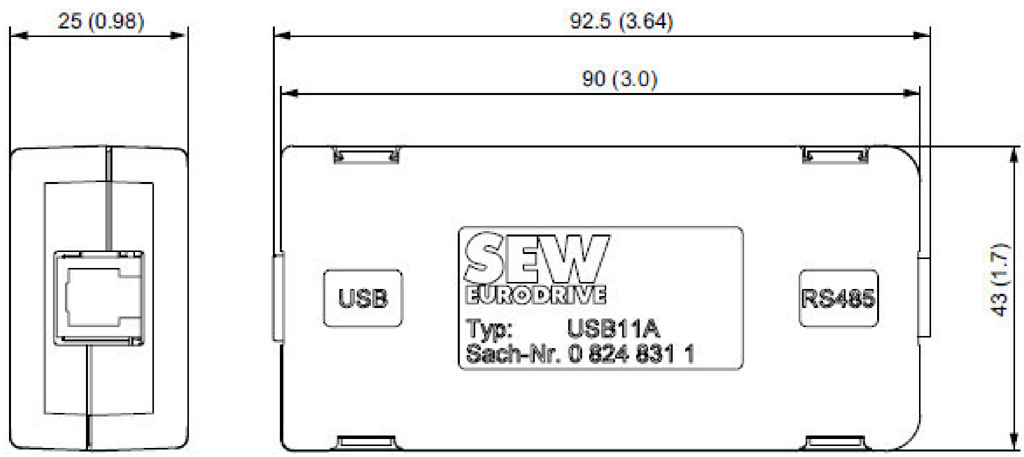


It is important to know how working both options due to some instances where computer is blocked; it is necessary to use key pad.

For constructing and assembling motor controller, it has all the necessary mechanical and electrical equipment. It is required to apply EMC protocol and thermal dissipation protocol taking into account operating process too.

For connections, it is used “16837703 MOVIDRIVE® MDX60B/61B Instrucciones de funcionamiento” and “11264926 MOVIDRIVE® MDX60B/61B Communication and Fieldbus Unit Profile” to learn operating and communication system. As others implementation stages, the most important here is to follow a safe and clean working in assembly stages to ensure the success.

After mounting, it is necessary install The MOVITOOLS®MotionStudio engineering tool to turn on electrical servo motor. As power supply, safety precaution is applied with insolation in each connection.

The MOVITOOLS®MotionStudio engineering tool from SEW‑EURODRIVE offers such a tool. With MOVITOOLS®MotionStudio, it can be parameterized, programmed, and diagnosed most of the inverter series from SEW‑EURODRIVE [13]. The features of this software are:

- Convenient drive startup and parameter setting.
- Drive diagnostics using the built-in oscilloscope function.
- Create application and user programs, in high-level languages if required, right on the plant floor using the Assembler or using the graphic programming interface.
- View the status of connected devices.
- Bus monitor.
- Control technology functions.
- Completed application modules for various applications.
- Read out electronic nameplates.
- Electronic nameplates of SEW ‑ EURODRIVE gearmotors are used for automatic motor adjustment MOVITOOLS®® MotionStudio supports engineering via:
    - Ethernet TCP/IP, PROFINET IO, EtherNet/IP, MODBUS TCP.
    - EtherCAT.
    - PROFIBUS DPV1, CAN, DeviceNet and the manufacturer-independent software interface TCI Tool Calling Interface.

In this case, it is used CAN communications.

When all is mounted, installed and checked, the first mechanical experimental test can turn on the electrical motor working with (no load and then coupled with the PMSM.

Here, it can be said it is finished third stage of verification.

## 3.5 dSPACE

MicroAutoBox is a real-time system for performing fast function prototyping in full pass and bypass scenarios. It operates without user intervention, just like an ECU. MicroAutoBox can be used for many different rapid control prototyping (RCP) applications such as power train, electric drives control, advanced driver assistance systems, etc.

MicroAutoBox can start up autonomously after power-up, with ECU-like boot-up times. A PC or notebook can be easily connected (hot-plugged) for application download, model parameterization, and data analysis via Ethernet. Application programs are stored in nonvolatile memory. MicroAutoBox contains signal conditioning for automotive signal levels and an integrated flight recorder for long-term data acquisition (incl. support of USB mass storage devices). Automotive Simulation Models works with MATLAB®/Simulink® models for real-time and offline simulation of:

- Components such as the engine, vehicle dynamics, and electrical systems.
- Passenger cars and trucks.
- Roads, maneuvers, and traffic scenarios.
- Modular simulation models for everything from component tests to virtual vehicle simulation.

For this thesis, the dSPACE hardware used is MicroAutoBox II 1401/1511/1512 where technical features are showed in Table 3.5.1 and Table 3.5.2.

Table 3.5.1 MicroAutoBox II 1401/1511/1512 technical details [18].

| PARAMETER | | SPECIFICATION |
|---|---|---|
| **MICROAUTOBOX II** | | **1401/1511/1512** |
| Processor | | IBM PPC 750 GL, 900 MHz (incl. 1 Mb level 2 cache). |
| Memory | | 16 MB main memory. |
| | | 6 MB memory exclusively for communication between MicroAutoBox II and PC/Laptop. |
| | | 16 MB nonvolatile flash memory containing code section and flight recorder data |
| | | Clock/calendar function for time-stamping flight recorder data. |
| Boost Time | | Depending on flash application size. Measurement examples: 1 MB size:160 ms; 3 MB size: 340 ms. |
| Interfaces | Host interface | 100/1000 Mbit/s Ethernet connection (TCP/IP). Fully compatible with standard network infrastructure. |
| | Ethernet real-time I/O interface | 100/1000 Mbit/s Ethernet connection (UDP/IP;TCP/IP). RTI Ethernet (UDP) blockset for R/W access. |
| | USB interface | USB 2.0 interface for long-term data acquisition with USB mass storage devices. |
| | CAN interface | 4 CAN channels. |

Table 3.5.2 MicroAutoBox II 1401/1511/1512 technical details (CONTINUATION) [18].

| PARAMETER | | SPECIFICATION |
|---|---|---|
| **MICROAUTOBOX II** | | **1401/1511/1512** |
| Interfaces | Serial interface (based on CAN processor) | 2 x RS232 interface. |
| | | 2 x serial interface usable as K/L-Line on LIN interface. |
| | ECU interface | 2 x dual-port memory interface |
| | IP module slot for FlexRay & CANFD | No available. |
| Programmable FPGA | | No available. |
| Analog Input | Resolution | 16 16-bits channels. |
| | Sampling | 16 parallel channels with 1Msps conversion rate. |
| | Input voltage range | 0 ~ 5V. |
| Analog Output | Resolution | 4 12-bit channels. |
| | Output voltage range | 0 ~ 4.5 V. |
| | Output current | 5 mA maximum. |
| Digital I/O | General | FPGA-based digital I/O. RTI software support for bit I/O, frequency and PWM generation / measurements. |
| | Bit I/O | 40 inputs.<br>40 outputs with 5mA output current. |
| | | Input/Output logic level: 5V or levels up to 40V (depending on Vdrive), selectable. |
| | PMW generation/ measurement | Channels fully configurable as frequency or PMW I/O.<br>PWM frequency 0.0003 Hz ~ 150 kHz, duty cycle 0-100 %, up to 21 bit resolution. |
| Onboard sensors | | Motion sensing with 3-axis accelerometer. Pressure sensing for altitude indication. |
| Signal conditioning | | Signal conditioning for automotive signal levels, no power driver included.<br>Overvoltage, overcurrent and short circuit protections. |
| Physical connections | | LEMO connectors for 2 ECU interfaces, Ethernet I/O interface, USB interface and Ethernet host interface.<br>Ethernet host interface (100/1000 Mbits/s, TCP/IP) for notebook/PC connection (for program load, experiment configuration, signal monitoring and flight recorder)<br>Integrated Ethernet switch. ZIF connector for I/O signals, mechanically secured, SubD connector for power supply. |

Real-Time Interface (RTI) is the link between dSPACE hardware and the development software MATLAB/Simulink/State flow from MathWorks®. The implementation time is greatly reduced. The hardware configuration for the real-time application is guided by automatic consistency checks to prevent parameterization errors.

The operating principle to work with RTI is the following: to connect the model to a dSPACE I/O board, just drag &drop the I/O module from the RTI block library and then connect it to the Simulink blocks. All settings, such as parameterization, are available by clicking the appropriate blocks.

Simulink Coder™ (formerly Real-Time Workshop®) generates the model code while RTI provides blocks that implement the I/O capabilities of dSPACE systems in Simulink models, thus preparing the model for the real-time application. The real-time model is compiled, downloaded, and started automatically on t real-time hardware, without the need of having to write a single line of code. RTI user guides during the configuration. RTI provides consistency checks, so potential errors can be identified and corrected before or during the build process [16].

Figure 3.5-1 dSPACE RTI to MicroAutoBox II.

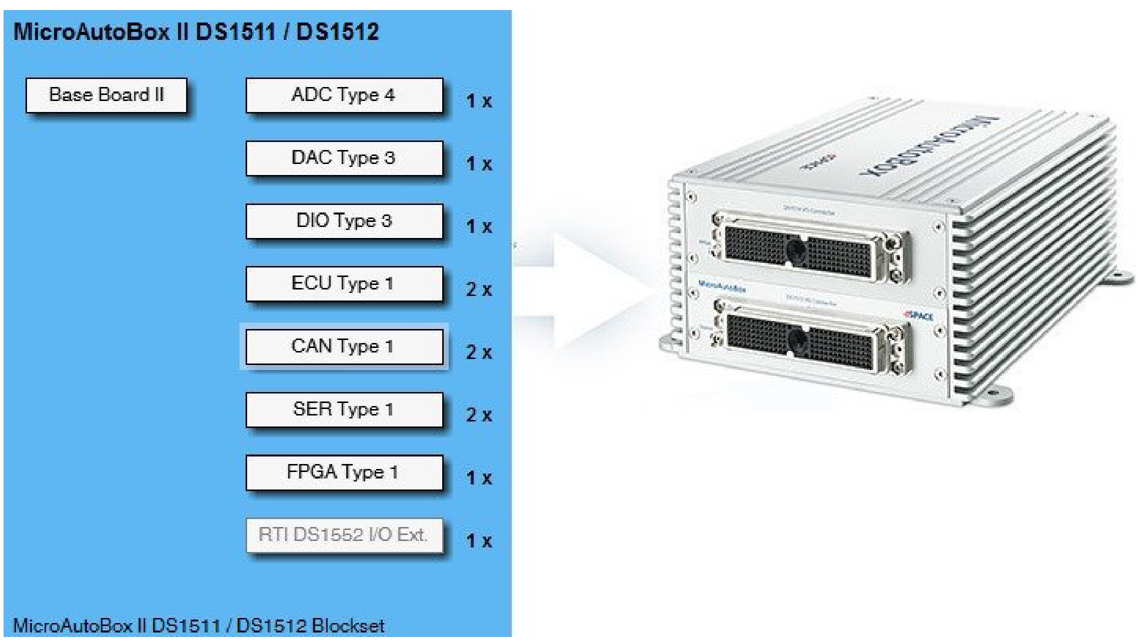


RTI can steer different channels at the same time allowing centralize in a single hardware whole system. RTI handles any kind of continuous-time, discrete-time, and multi-rate system. Depending on the I / O hardware, different channels of the same I / O board can be used formally different sample rates, and even in different subsystems.

Also it supports time-triggered tasks and timetables, which allow to the implement tasks and groups of tasks with varying delay times or predefined in relation to an associated trigger event makes this task handling in flexible model. In Addition, RTI offers which checks help avoid double or improper use of channels.

In our case, we are using 3 connections, 2 CAN which handle motors and one more to measure PMSM behavior. When the application is running on the real-time hardware, the whole dSPACE experiment software is at the disposal. These connections are cables that comply with EMI and electrical requirements.

RTI ensures that the control over each individual variable immediately after the implementation process. ControlDesk Next Generation provides an instrument panel that enables changes in parameters and monitor signals –without regenerating the code. It also displays the time histories of any variable used by the application [17].

# Chapter Four

# 4 Electric Vehicle Model

## 4.1 Parameters

For this thesis, it is required a model of the electric vehicle for the experimental test. Continuing the research project VEIL from ISEC, the diesel vehicle converted to electric vehicle had the following characteristics [18]:

- Manufacturer: LIGIER.
- Model: 162GL.
- Engine: LOMBARDINI.
    - Type: 4 times.
    - Fuel: Diesel atmosphere.
    - Cylinder: 505 cc.
    - Output power: 5.4 CV.
    - Speed: 3100 rpm.
    - Maximum Torque: 15.1 Nm at 2340 rpm.
- Dimensions: 2.45x1.40x1.50 m.
- Weight: 350 kg.
- Weight engine: 60 kg.
- Wheels: 145/70/R13 (r=0.26 m).
- Maximum speed: 45 km/h fixed by EU legislation.

When the conventional internal combustion engine and corresponding systems were retired and it is considered the test bench batteries electric motor, motor controller and some other components, the vehicle mass, m, is 500 kg considering average weight from driver.

## 4.2 Dynamic model

The dynamic model is extracted from VEIL documentation [19]+[20]. If the forces that oppose the vehicle movement are drawn in a scheme in Figure 4.2-1, it can be seen: the rolling resistance force of proper tires to the tire-road contact, $F_{rr}$; the aerodynamic drag force, $F_{ad}$; the resultant force of the slide movement on a plan inclined road, $F_{hc}$.

Depending on the type of travel of the vehicle (rising or falling), $F_{hc}$ can be resistant to the movement or in its favor.

Where there is change in the vehicle speed, the force required to provide linear acceleration of the vehicle mass $F_{la}$ and the force needed to angular acceleration of the rotating masses (wheels , mechanical transmission motor rotor) $F_{wa}$ should be considered.

**Figure 4.2-1 Force distribution for electric vehicle.**

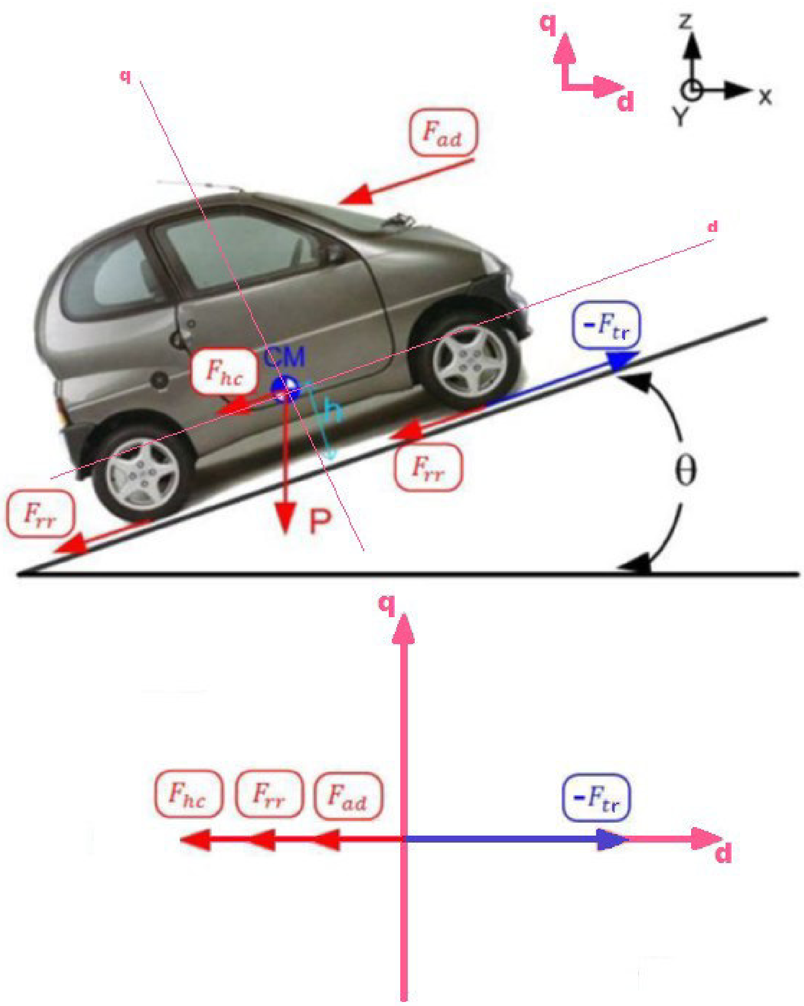


Therefore, the total resistive force $F_{tr}$, to movement of the vehicle, is the vector sum of the resistant forces which act on it, as indicated in (1).

$$F_{tr} = F_{rr} + F_{ad} + F_{hc} \qquad (1)$$

At low speeds and presence of hard surfaces, the opposed to vehicle movement is mainly due to the component rolling resistance force, which is far superior to aerodynamic drag force ($F_{rr}$>>$F_{ad}$). For higher speeds the main force resistant to movement is aerodynamic drag force.

The resultant force of road gradient $F_{hc}$, is a function of tilt angle tetha and independent of speed and floor type and presenting positive values when it is positive (rising) or negative when negative (falling).

The rolling resistance force, expressed in (2) is the sum of the rolling resistance forces at each wheel, and function of the rolling resistance coefficient and vehicle mass. The value of this coefficient can be easily determined by measuring the force required to pull the vehicle with a very low constant speed. Typical values vary between 0.015 for conventional tires and tires specifically designed to 0.005 for electric vehicles. In this case, conventional tires are used, so the constant is 0.015.

$$F_{rr} = \mu_{rr} \cdot m \cdot g \qquad (2)$$

For other hand, the air resistance is proportional to the density of the air, the drag coefficient (drag Coefficient), the front area of the vehicle, and the relative wind speed of the vehicle squared, as expressed in (3).

$$F_{ad} = 0.5 \cdot \rho \cdot C_d \cdot A_f \cdot v^2(t) \qquad (3)$$

Where:

- Air density to 25ºC: $\rho = 1.16$ kg/m$^3$.
- Drag coefficient: $C_d = 0.51$.
- Front area: $A_f = 2.1$ m$^2$ (Product height and width of the vehicle).
- Speed wind relative to the vehicle: $v \quad (t)$ m/s.

Therefore, the power required at the vehicle, necessary to overcome aerodynamic drag increases with the cube of speed, as shown by (4). It should also be noted that the air density is a function of air pressure and air temperature.

$$P_{ad} = F_{ad} \cdot v \qquad (4)$$

Finally, the resultant force of the slide movement on a plan inclined road depends on the vehicles mass, m, and road angle to the horizontal thetha being calculated as shown in (5).

$$F_{hc} = m \cdot g \cdot \sin\theta \qquad (5)$$

In torque terms, each torque must be referred to the motor shaft and adding them to generate total resistant torque. Remembering that

$$T = F \cdot r \tag{6}$$

the torque that the PMSM motor should provide, Tm, is given by (7).

$$T_m = T_{r_m} + T_{a_m} \tag{7}$$

where:

- $T_{r_m}$ : Torque from resistant forces, $F_{tr}$ (1), in the motor referential.
- $T_{a_m}$ : Torque to accelerate the vehicle mass and the rotating masses, in the motor referential.

Considering that the torque from resistant forces at the wheels, $T_{r_w}$, is

$$T_{r_w} = F_{tr} \cdot r\,; \tag{8}$$

$T_{r_m}$ is given by (9).

$$T_{r_m} = F_{tr} \cdot r \cdot \left(\frac{1}{\eta_{gb} \cdot i_{gb}}\right) \tag{9}$$

The torque due to the masses acceleration, $T_{a_m}$, is given by (10),

$$T_{a_m} = J_T \cdot \dot{\omega}_m \tag{10}$$

with the total moment of inertia, $J_T$, in the motor referential, given by

$$J_T = J_w + J_m + J_v \tag{11}$$

where:

- $J_w$: Moment of inertia of wheels, propeller shaft.
- $J_m$: Moment of inertia of motor, flywheel and clutch.
- $J_v$: Moment of inertia of the vehicle.

This means that to calculate the total moment of inertia referred to the motor shaft, it should be considered all the different moments of inertia affecting the electric vehicle.

Due to lack of information of a few parameters of the vehicle, it was decided to neglect $J_w$ and $J_m$ because they are negligible with respect to moment of inertia of the vehicle. It can be said that the total moment of inertia is approximately to the vehicle moment of inertia seen from the motor like shown in (13).

$$J_T = J_w + J_m + J_v \approx J_v \tag{12}$$

The moment of inertia corresponding to vehicle mass at the wheels, $J_{v_w}$ is

$$J_{v_w} = m \cdot r^2 \tag{13}$$

and so, the moment of inertia corresponding to vehicle mass in the motor referential, $J_v$ is

$$J_v = m \cdot r^2 \cdot \left(\frac{1}{{i_{gb}}^2 \cdot \eta_{gb}}\right) \tag{14}$$

To understand (13), it is necessary to remember that the linear acceleration force, $F_{la}$, to provide the linear acceleration of the vehicle mass is obtained by Second Newton Law as in equation (15),

$$F_{la} = m \cdot \frac{dv(t)}{dt} = m \cdot r \cdot \frac{d\omega_w}{dt} = m \cdot r \cdot \dot{\omega}_w \tag{15}$$

Considering (6), it can be seen that:

$$T_{la} = F_{la} \cdot r = m \cdot r^2 \cdot \dot{\omega}_w = J_{v_w} \cdot \dot{\omega}_w \tag{16}$$

So, an electric motor torque must be able to support the different efforts in real time demanded by the road and to accelerate the masses, in this case, imposed by the servomotor that will emulate the road and accelerations. Finally, the motor mechanical power, $P_{mm}$, is given by (17).

$$P_{mm} = T_m \cdot \omega_m \tag{17}$$

## 4.3 Implementation / Simulation

The test bench is built under a mobile metal chassis to facilitate the user's work. This consists of three main parts defined as levels. At the first level the power supply is located. The batteries pack with the battery management system and lithium battery charger as shown in Figure 4.3-1 [6] [7].

Figure 4.3-1 Level 1. Power supply

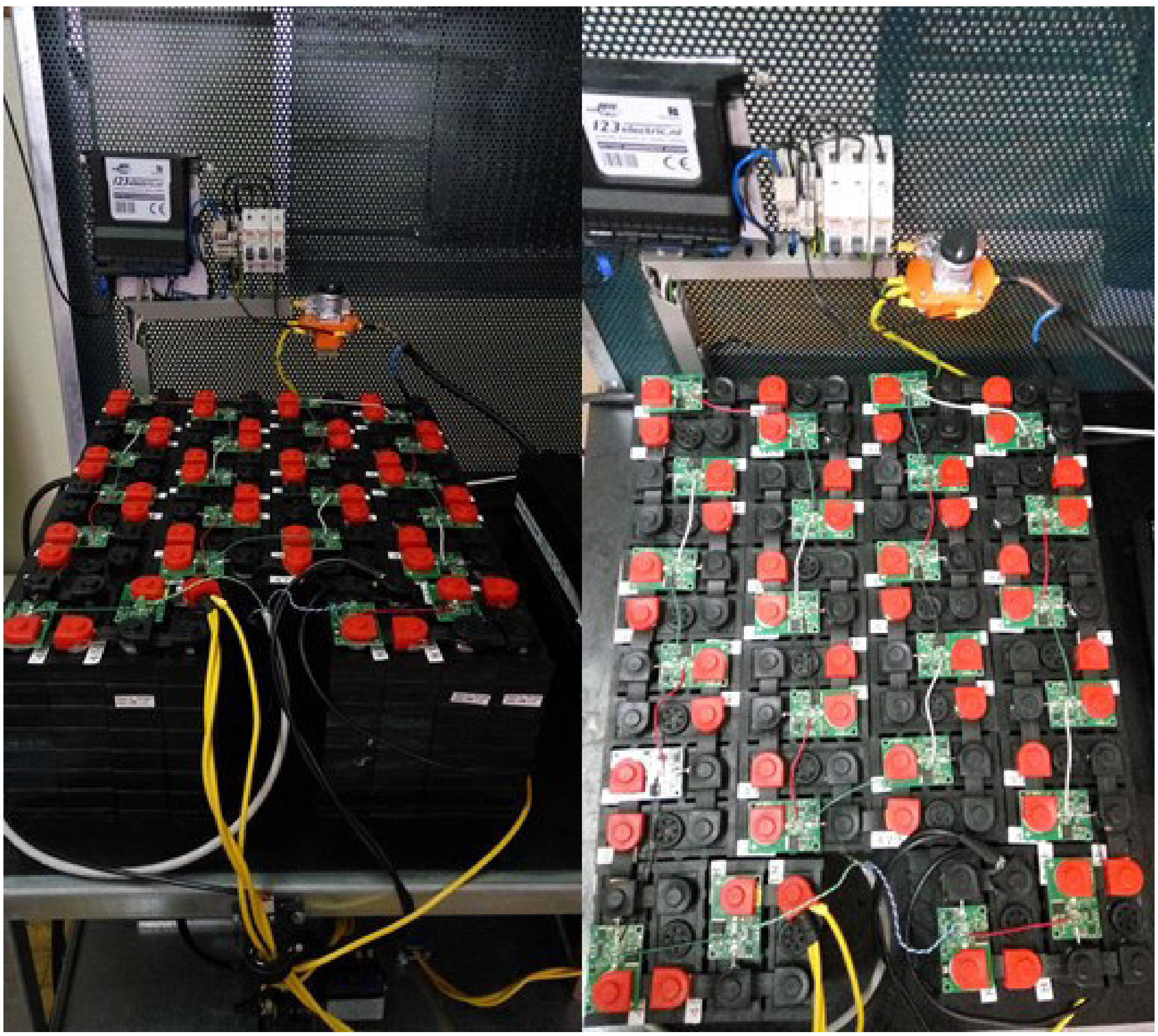

On the level 2, the motor controllers are located, SEVCON with the electromechanical contactor and dSPACE as shown in Figure 4.3-2 [10],[11],[17]. It can also be seen a DC/DC converter and an inductor that are incorporated for future power management works.

Figure 4.3-2 Level 2. Motor Drivers.

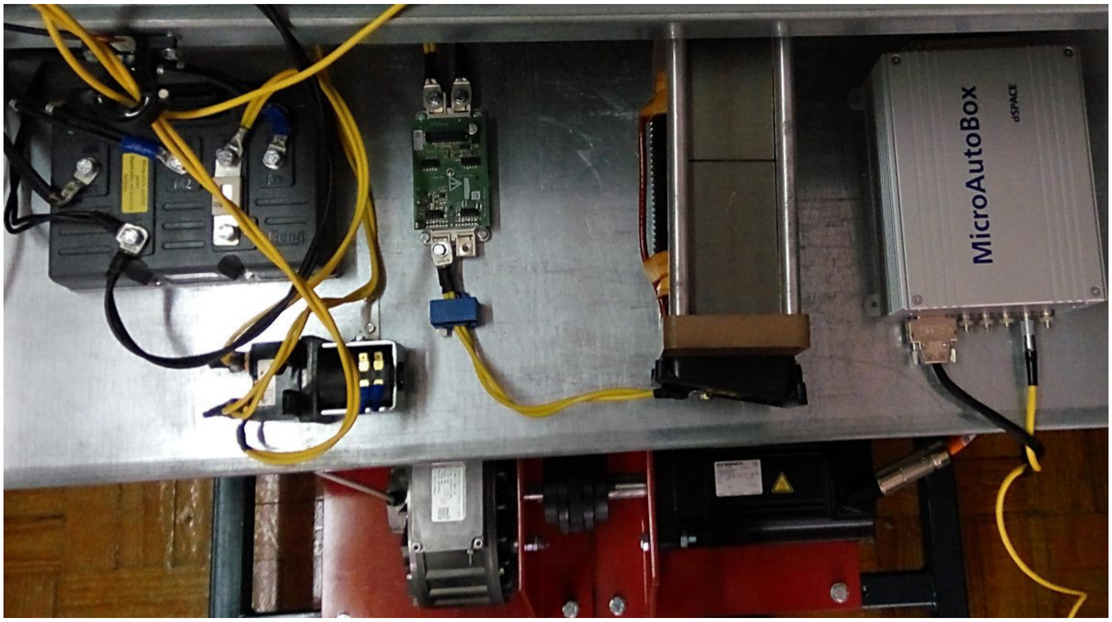


On the third level, on a second moving surface, the motors are located, the electric traction motor and servomotor, as shown in Figure 4.3-3[21], [22].

Figure 4.3-3 Level 3. Electric Motor and Servo Motor.

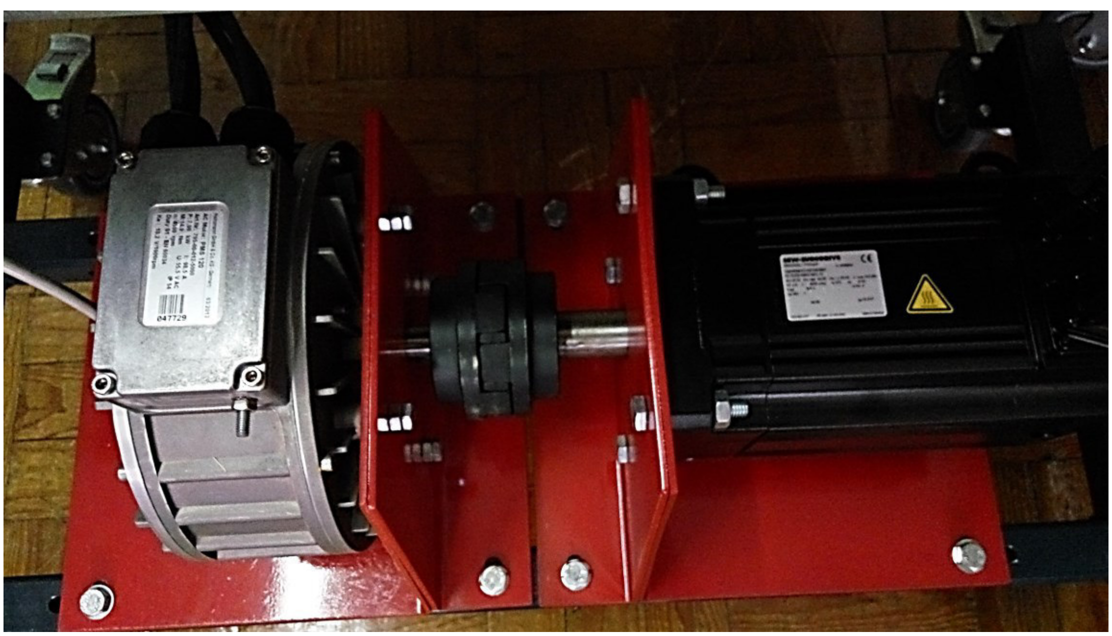

Besides these main levels, there are two other secondary but also important. The vertical plate that facilitates the installation of terminals and ground (earth) conductor terminal blocks, plugs safety and servo motor controller. As the second part, it would be the back of the vertical plate where the heat sink of the servomotor is breaking energy resistor is placed as it can be seen in Figure 4.3-4 [13],[22].

**Figure 4.3-4 Secondary Levels. Vertical plate: frontal and back.**

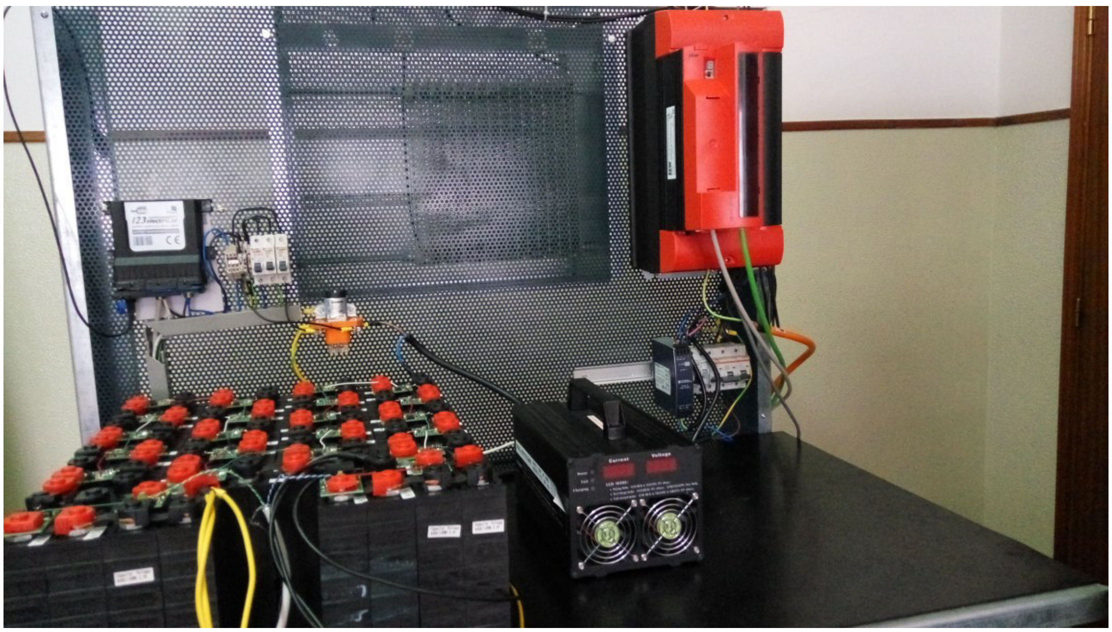

Three experimental trials have been carried out before the final test. These experimental trials were performed throughout implementation to ensure its electromechanical operation.

The first electromechanical trial, as discussed in the previous chapter, was a test operation of the electric motor with selector blocks operating full mechanically [21].

As second electromechanical trial, also commented in the previous chapter, the servomotor and drive behavior was tested with manufacturer software enclosed with this product by DVT SEVCON Software [14].

*All electromechanical tests were performed under the supervision of the thesis supervisor and project assistant following security protocols to ensuring safety and success of the tests.*

A third electromechanical & computer trial was with dSPACE. It consists in 3 basic tests through Simulink tool to ensure transmission and response data through this product [17].

- The first test consisted in transmitting a signal through dSPACE to multi-meter.
- The second test consisted in the reception of a signal from a variable voltage source.
- The third test consisted in transmitting and receiving data trying to control both previous circuits at same time.

Figure 4.3-5 shows Simulink model used for the third test in dSPACE hardware.

Figure 4.3-5 Basic trial in Simulink tool to dSPACE communication.

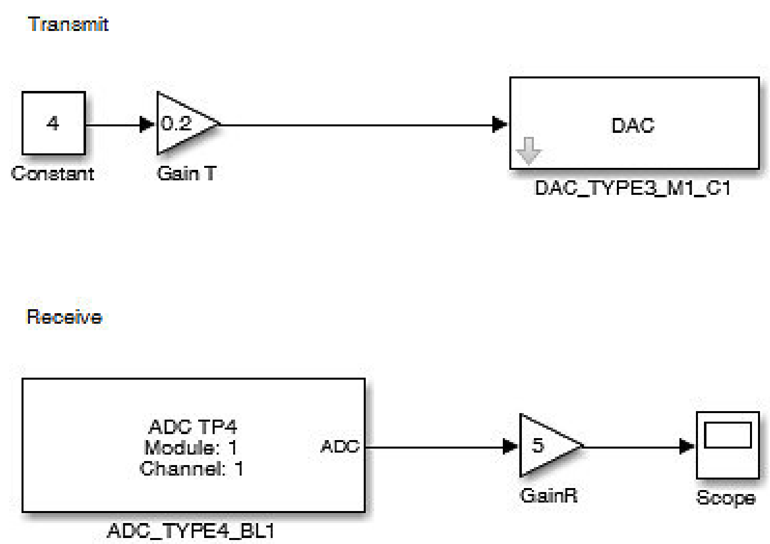


After these experimental trials, the connections between motors and controllers were altered to add dSPACE to govern both motor from the ControlDesk interface. To do this, it is necessary to build a preliminary model in Simulink. It will be so complex due to motors communications are through CAN so it is necessary to programming code.

The communications development consists in listen CAN communication for each motor controller and check which are the messages that each drive is using to communicate with each motor, check RTI CAN block set from dSPACE in Simulink tool and build the model the link with them.  This work depends on the motor wanted to be tested while the servomotor is always fixed. Finally, the full test bench is controlled by dSPACE.

In order to ensure correct operating of test bench, it is necessary following operating protocols which allows to be analyzed with another tests before completed. For that, the electric motor should be subject to the demands of determined protocol. There is a reference book of driving cycles for use in the measurement of road vehicle emissions. Taking into account EU legislative cycles program and characteristics of electric vehicle, it was chosen ECE 15 cycle driving which have the following parameters.

- Distance: 1017 m.
- Duration: 195 s.
- Average speed: 18.83 km/h (5.23 m/s).

Figure 4.3-6 shows the speed and the acceleration that is subjected in the PMSM.

**Figure 4.3-6 ECE-15 curves subjected [23].**

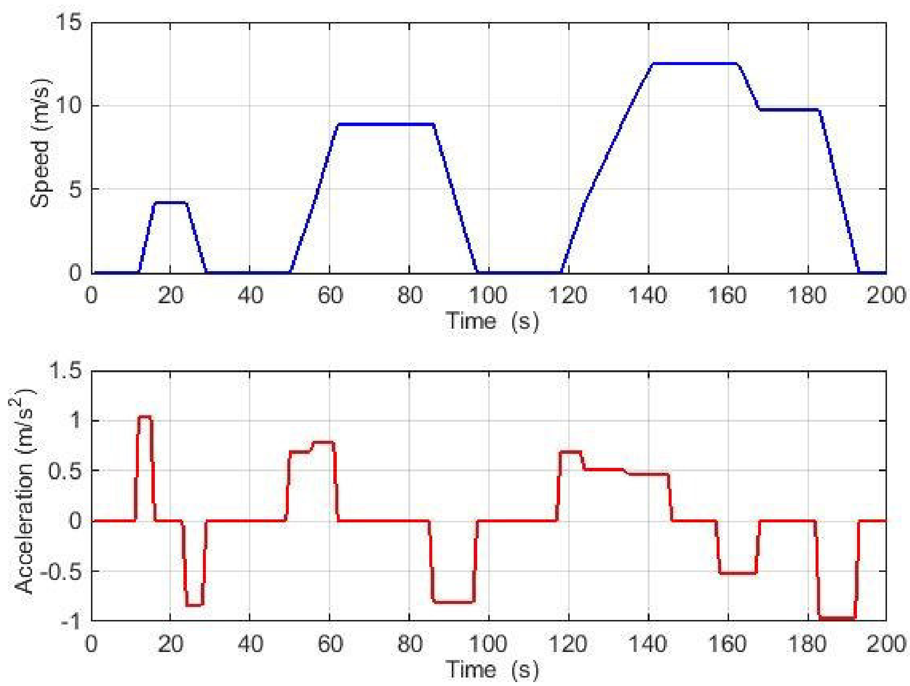


Mathworks Inc. also offers a driving cycle block to Simulink implementation. These block facilities predetermined driving cycles for our test bench. Closing the equations from the previous chapter, the mechanical power to be supplied by the electric motor can be calculated theoretically as shown in Figure 4.3-7.

Figure 4.3-7 ECE-15 requirements.

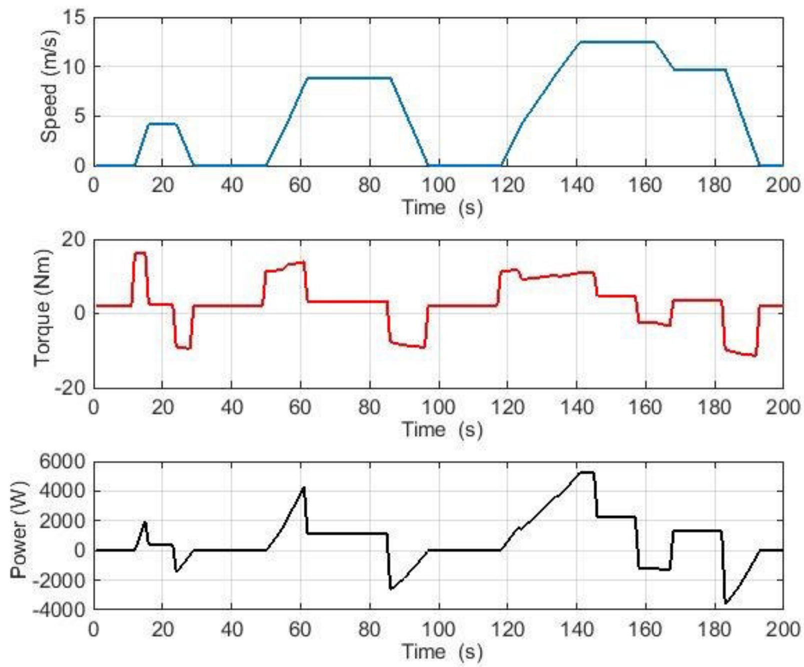


The reference speed imposed by the ECE 15 driving cycle to the electric motor can be seen in top plots. In the second plots level appears the resistant torque that the servomotor apply to the traction motor (corresponding to $T_m$, the sum of $T_{rm}$.plus $T_{am}$ ). Third plots level shows the mechanical power, $P_m$, necessary to complete ECE 15 driving cycle.

To have better in sight, torque and power values are broken down in electrical and mechanical, resistance and acceleration. Figure 4.3-8 and Figure 4.3-9 respectively.

- $P_{mm}$: Motor Mechanical Power.
- $P_{mw}$: Wheel Mechanical Power at the wheel.
- $T_m$: Motor Torque.
- $T_{rm}$: Resistant Torque from force independent from acceleration.
- $T_{am}$: Resistant Torque from force dependent from acceleration.

For other hand, the Figure 4.3-10 shows the relationship between the electric motor speed (in rpm), N, given by (22), and the lineal speed of the electric vehicle in order to allow motor control.

$$\omega_m = 2 \cdot \pi \cdot N \quad (18)$$

Considering that the wheel angular speed, $\omega_w$, is equal to (19),

$$\omega_w = v/r \qquad (19)$$

and can be related to the motor angular speed, $\omega_m$, by (20),

$$\omega_m = \omega_w \cdot i_{gb} \qquad (20)$$

from (15), the motor speed in rps is given by (18).

$$N_m = \omega_m \cdot \frac{1}{2\pi} = \omega_w \cdot i_{gb} \cdot \frac{1}{2\pi} \qquad (21)$$

and the motor speed in rpm, N, is given by (19).

$$N = 60 \cdot N_m \qquad (22)$$

Finally, some of the most representative values for the motor are presented in Table 4.3.1; it can be see how the power imposed by ECE 15 driving cycle is smaller than nominal output power of the traction electric motor in the following critical points.

**Table 4.3.1. Values for ECE 15 driving cycle.**

| PARAMETER \ POINT | UNITS | 141 S | 150 S |
|---|---|---|---|
| Power mechanical motor | kW | 5.29 | 2.24 |
| Power mechanical wheel | kW | 5.03 | 2.13 |
| Speed motor | Rpm | 4591 | 4591 |
| Torque motor | Nm | 10.8 | 4.67 |

**Figure 4.3-8 ECE-15 Power curves.**

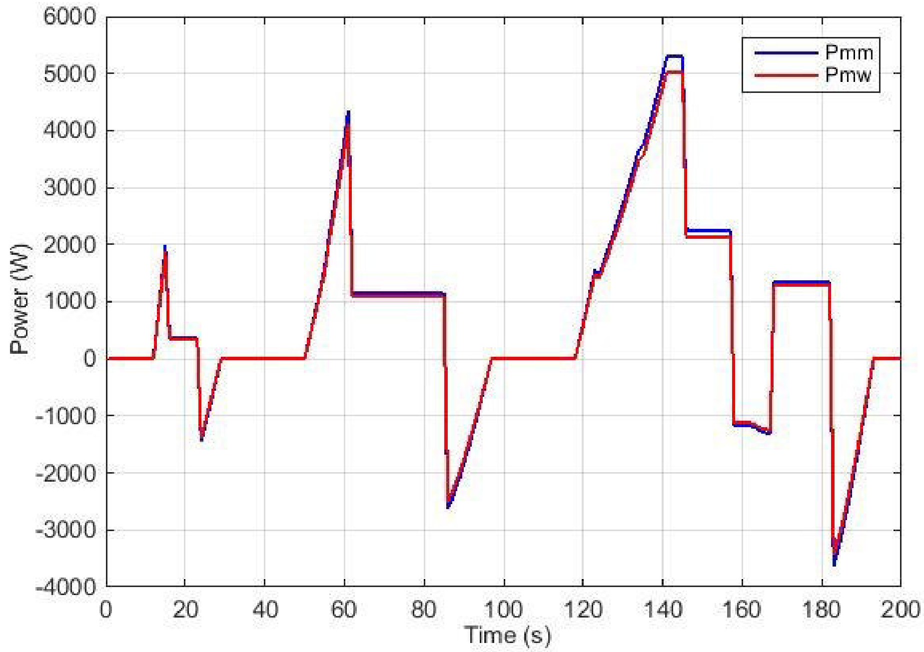


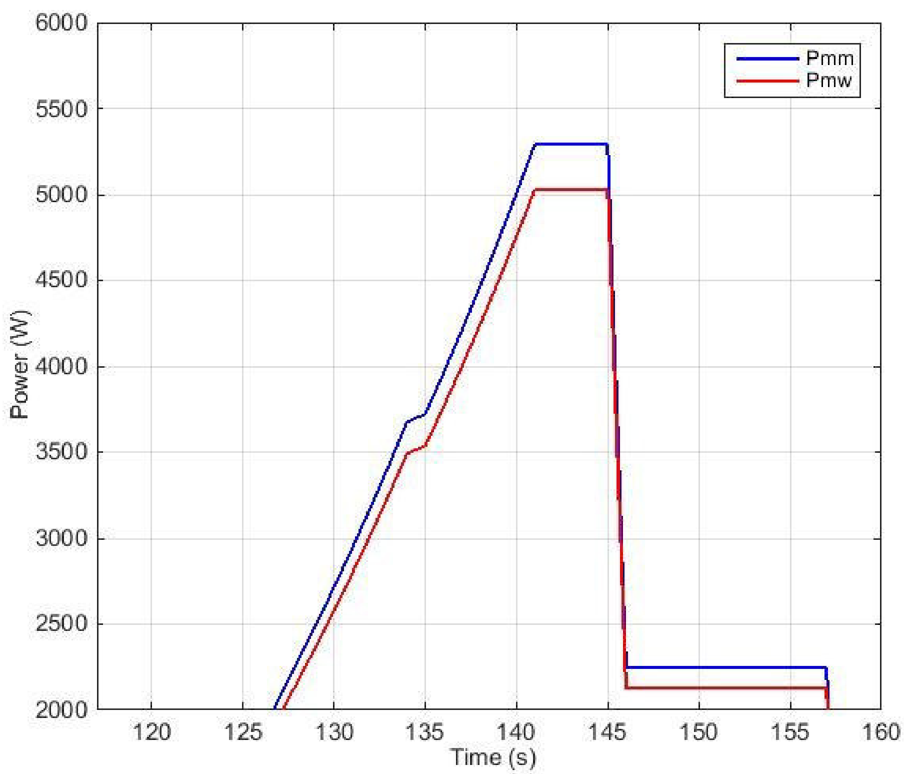

Figure 4.3-9 ECE-15 Torque curves.

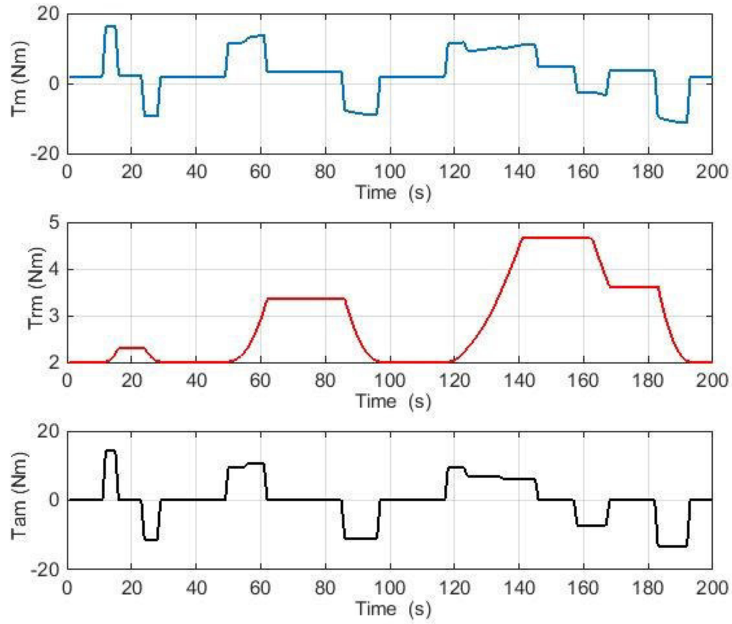


Figure 4.3-10 Relationship between EV linear speed and motor speed.

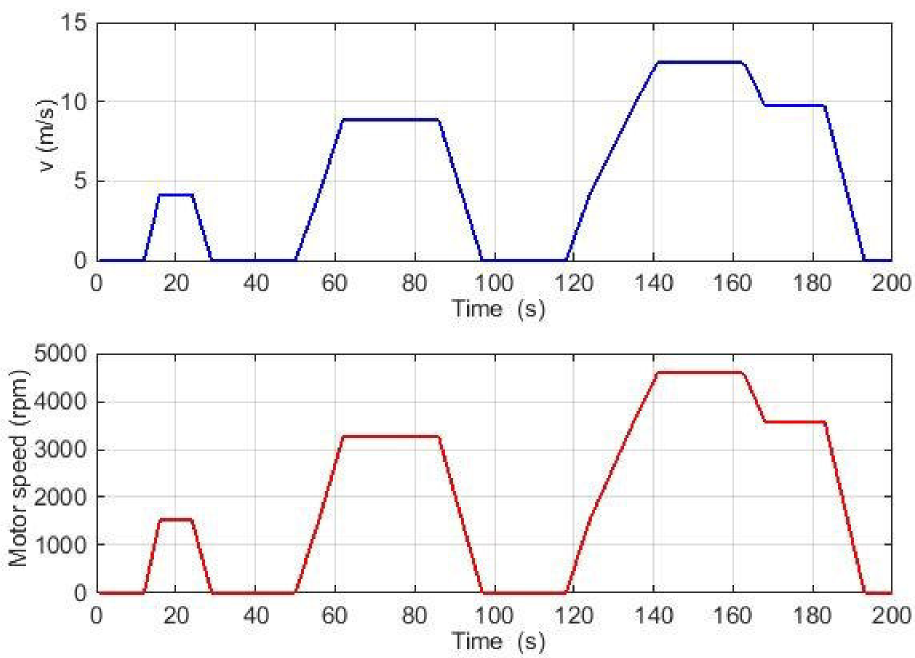

## 4.4 Evaluation with electric motor properties

Through the Hardware Setup Detail and Electric Vehicles Mode, presented in Chapter 3 and 4 respectively, it has been concluded that PMS 120 electric motor from HIENZMANN manufacture complies with the mechanical and electrical requirements subjected by ECE 15 driving cycle.

If the results are compared with the previous work done in the ISEC, it can be seen that the results have similar orders but do not exactly match them. This is due to the following aspects.

### 4.4.1 Parameters

The parameters taken in the present work and reference for the electric vehicle dynamic model are not exactly the same due to the variety of alternatives values of each variable like, air density, car mass, inertia moment, etc. [19]+[24].

### 4.4.2 Driving cycles

If the work cycles are analyzed, it can be seen that although both are ECE 15 driving cycle however they have different technical characteristics. In the work of the ISEC [19][24], they are based on the points of the European Union and the workbench are taken into account Simulink blocks provided by Mathworks & Cranfield University Figure 4.4-1 shows ECE 15 distribution times and gear box stage [25].

Figure 4.4-1 ECE 15 distribution times and gear box stage [27].

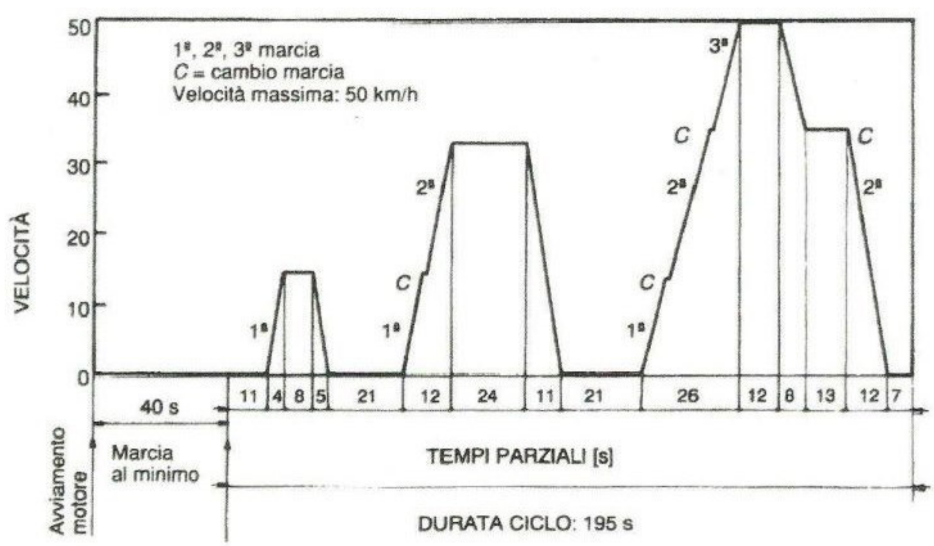

If the large motor development is chosen at 117 s, it can be seen that the car slowly accelerates to 50 km/h (12.5 m/s) in 26 seconds, the distribution in manual is: 5 s, 9 s and 8 s in the 1st, 2nd and 3rd gears, with additional 2 × 2 s for gear changes.

For other hand, the Figure 4.4-2 it can be see how slope is different, the distribution time to gear changes is less than UE case, 1.5 s between 1st, 2nd gears and bit less 1 s between 2nd and 3rd gears.

Figure 4.4-2 ECE 15 distribution times and gear box stage by Cranfield University.

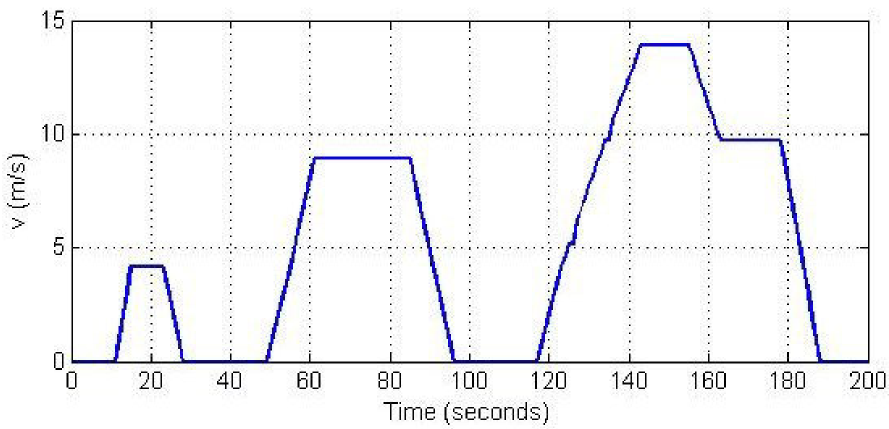


As additional case, VEIL researchers modified the driving cycle reducing the 26 s acceleration period on the 3rd start from 26 s to 8 s, in order to get maximum effort for electric motor as shown Figure 4.4-3.

Figure 4.4-3 ECE 15 power demand and available regenerative power on the wheels and on the power sources [23].

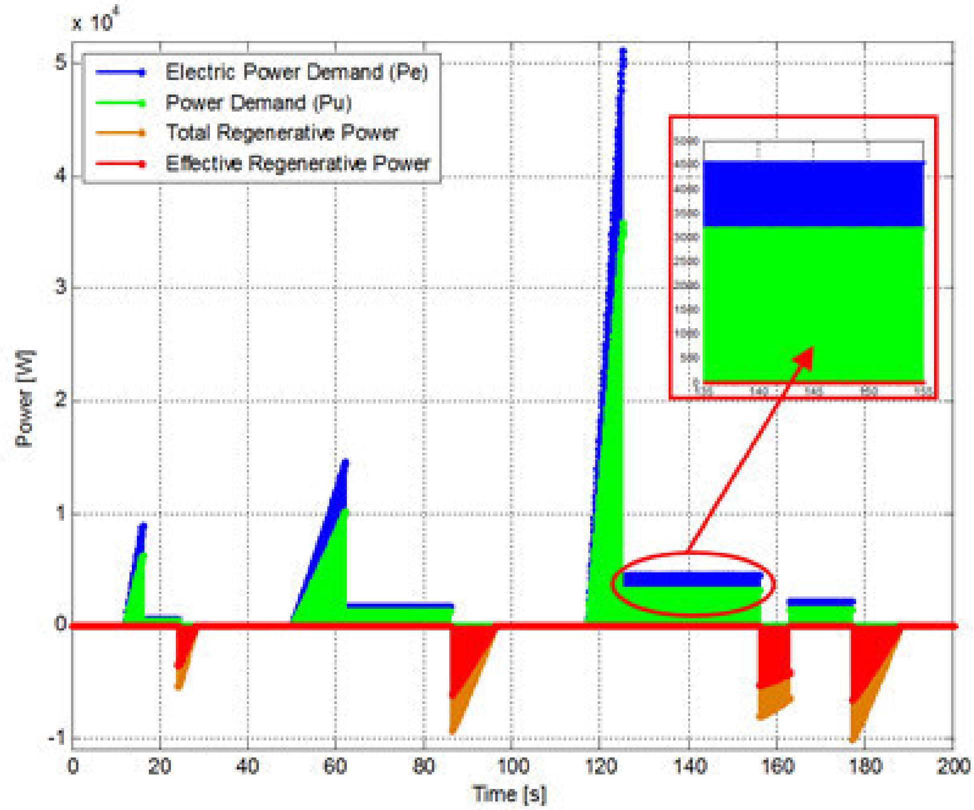


If the average acceleration is calculated, (13) corresponds with Figure 4.4-1, (14) correspond with Figure 4.4-2 and (15) with Figure 4.4-3 respectively.

$$\bar{a}_{ISEC} = \frac{dv}{dt} = \frac{\Delta v}{\Delta t} = \frac{14-0}{143-117} = 0.5385\ m/s^2 \qquad (13)$$

$$\bar{a}_{testbench} = \frac{dv}{dt} = \frac{\Delta v}{\Delta t} = \frac{12.5-4.167}{143-126} = 0.4902\ m/s^2 \qquad (14)$$

$$\bar{a}_{modified} = \frac{dv}{dt} = \frac{\Delta v}{\Delta t} = \frac{14-0}{126-117} = 1.75\ m/s^2 \qquad (15)$$

### 4.4.3 Electric Vehicle Maximum Speed

EU Regulation on the Approval of L-Category Vehicles state that Light quads of VEIL must be limited by manufacturers at 45km/h as maximum speed [26].

## 4.5 Conclusion of the chapter

This thesis has been at the height of the technological revolution that we are living today. Changing the conventional world to renewable energies and ending use of fossil fuels makes it a revolution.

This thesis gives the necessary knowledge of understanding the basic electric vehicle operation, the different parts that form it and how work them as separately as together. In management thesis division, the knowledge that projects always are linked to previous scientific work done, there are too many alternative for implementation of electric vehicle, but as a counterpart, there is a trouble of operating protocols among manufacturers.

In this case, manufacturer's contact has generated slowed work and walls during the implementation, not letting motor performance in real time simultaneously coordinated by dSPACE. Moreover, there was some studying and working with existing wiring, which has led to use electrical coding using signals in the terminals and to detect and repair some wires with bad electric contacts. The design and calculations of the study of a small electric car was relatively easy because it was decided to opt for the experimental vehicle VEIL located in ISEC.

Chapter five

# 5 Conclusions and Outlook

This chapter presents the main conclusions reached out of the work, and puts the light on the main covered issues and the present work situation. Then an outlook is proposed for the future work.

## 5.1 Conclusions

This thesis has managed to study and improve some wiring of a test bench allowing emulating in hardware a small electric vehicle behavior, formed by the batteries, controllers, electric motor and driving cycles that it has to be overcome before being marketed. Considering these aspects it can be concluded that:

- The $LiFePO_4$ batteries are best offer theoretical and practically yield for electric automotive today.
- The motor drivers have to overcome technological barriers between manufacturers and set a minimum common protocol tools in order to establish compatibility. It is not a crazy idea because this happening in others fields, i.e. the telecommunication field, was established a universal USB micro cable to smartphones.
- As a final step, the PMSM motors are a good choice for electric automotive, provide good performances; although it has been thought about, debated and researched among different members from ISEC, the option of placing one electric motor at each wheel under one unique control (dSPACE), this would give traction higher order and improve more than the power of the electric vehicle.

## 5.2 Future Work

As a next step of this thesis, it is necessary to go upstream of the electric motor, to search for the autonomy. Perform charge / discharge cycles of the batteries system pack and see how batteries system behaves under driving cycles required by European Union. After the electric vehicle behavior analysis is completed, it could move the model to the VEIL vehicle where it could be implemented and studied the real behavior of the electric vehicle.

# References


[1] U. S. Department of Energy, “Office of Energy Efficiency & Renewable Energy,” 2015. [Online]. Available: http://energy.gov/eere/transportation. [Accessed: 17-Jun-2016].

[2] M. Scott, D. Hopkins, and J. Stephenson, “Understanding sustainable mobility: The potential of electric vehicles,” in *Proceedings - IEEE International Conference on Mobile Data Management*, 2014, vol. 2, pp. 27–30.

[3] Fermin Soneira Santos. SEAT, “Hybrid Control Systems. Lesson 3 – Electromobility,” Introduction Course - EECPS Master Degree. University of Oviedo. 2013.

[4] Sinopoly. Batteries Manufacturer, “Sinopoly Lithium Ion Battery Secification of model: SP-LFP40AHA,” p. 80. 2016.

[5] D. R. Tobergte and S. Curtis. GWL/Power Group Technology Solutions “POW72V35A/BMS CHARGER SPECIFICATION,” *J. Chem. Inf. Model.*.vol. 53, no. 9, pp. 1689–1699, 2013.

[6] S. T. Mems. GWL/Power Group Technology Solutions. “BMS123 COMMUNICATION PROTOCOL,” no. January, pp. 1–26, 2012.

[7] HEINMANN. Group. PERM Technology “PRODUCT CATALOGUE Disc Motors.”. p. 15. 2016.

[8] SEVCON. A. C. M. Controller, “SEVCON Gen4. AC Motor Controller”. 2015.

[9] S. S. Controller and C. Diagram, “Motor Controller for Permanent Magnet AC-Synchronous Motor ( Axial Flux Motor ) Gen4 Sevcon Controller Setting-Up Sevcon Controller Connection Diagram.”

[10] S. Jetscan and J. Speed, “DVT. SEVCON GEN4,” vol. 44, no. 0, p. 240, 1997.

[11] I. Note, O. N. The, E. Version, L. The, and E. Projects, “SEVCON Gen4 Application note. Adding PDOs,” vol. 44, no. 0, pp. 1–2, 2010.

[12] I. Note, O. N. The, E. Version, L. The, and E. Projects, “SEVCON GEN4. Application note. PDO Fundamentals App,” vol. 44, no. 0, pp. 1–2, 2010.

[13] I. G. Units, D. Electronics, and D. Automation, “MOVIDRIVE ® MDX60B/61B Communication and Fieldbus Unit Profile,” 2009.

[14] I. G. Units, D. Electronics, and D. Automation, “MOVIDRIVE ® MDX60B/61B Drive Inverter. Operating Instructions, 1122 2913/ EN” 02/2004.

[15] I. G. Units, D. Electronics, and D. Automation, “MOVIDRIVE ® MDX60B/61B Drive Inverter. Technical data,” 2007.

[16] dSPACE. GmbH, “Real - Time Interface,” pp. 56–61, 2016.

[17] dSPACE. GmbH, “MicroAutoBox II" total pages 574. 2016”.

[18] L. Services, “Lombardini LDW 502 Automotive. Manual,” no. May, pp. 1–98, 2005.

[19] VEIL project, “VEIL Vehiculo Electrico Isento de Licença,” Project VEIL wiltage, 2013, Departamento Engenharia electrotécnica. ISEC, http://www.dee.isec.pt/veil/.

[20] J. C. P. Palma, Accionamentos electromecânicos de velocidade variável, Fundação Calouste Gulbenkian, Lisboa, 1999.

[21] R. Saint Simon, “SEVCON GEN4 Applications reference manual 177/52701 v3.3.” 2015.

[22] H. Gmbh and E. Drives, “synchronous disc armature motors ( axial flow motor ) PMS model series Installation instructions,” 2012.

[23] T. Barlow, S. Latham, I. Mccrae, and P. Boulter, “A reference book of driving cycles for use in the measurement of road vehicle emissions,” p. 280, 2009.

[24] J. P. F. Trovao, “Optimização e Gestão de Múltiplas Fontes de Energia em Veículos Eléctricos”. Tese Doutoramento. FCTUC Faculdade de ciencias e tecnologia. Univrsidade de Coimbra. Outubro 2012.

[25] The Car Repairing Community, “Autodiagnostic,” 2015 [Online]. Available. http://www.autodiagnostic.it/2014/03/17/consumi-dichiarati-dalle-case-assolutamente-irreali/ .

[26] A. Burrows, “EU Regulation on the Approval of L-Category Vehicles,” no. December, 2013.

# APPENDIX

## A.1.- Matlab script

```
% Simulation and Full-Scale Emulation of a Powertrain for Small Electric Vehicle
% Variables
g = 9.8;        % [kg * m/s2] Gravity Force
m = 500;        % [kg]  Small EV + batteries + driver. Reference thesis
urr = 0.015;    % [-]   Rolling resistance coefficient. Reference thesis
Cd = 0.51;      % [-]   Drag coefficient. Reference thesis
Af = 2.1;       % [m2]  Front area of the vehicle
r = 0.26;      % [m]   Wheels radius
igb = 10;       % [-]   Ratio gear box
ngb = 0.95;     % [%1]  Eficiency's Gear Box
rho = 1.16;     % [kg/m3] Air Density 25°C
teta = 0;       % [deg] slope
%%
sim('Curves_ArtUrban.slx');
%sim('cycle_ECE');
%%
% Total resistant force Ftr
Frr = urr * m * g;                        % (2)defined urr before
Fad = 1/2 * rho * Af * Cd * v.^2;         % (3)defined rho before
Fhc = m * g * teta;                       % (4)defined teta before
Ftr = Frr + Fad + Fhc;                    % (1)resistant forces
Trm = Ftr  * r * 1/ (igb * ngb);          % (10)Torque resistant torques


ww  = v / r;                              % (16) rad/s angular speed wheel
Dww = dv/ r;                              % angular acceleration at wheel
Dwm = Dww * igb;                            % angular acceleration at motor
wm  = ww * igb;                             % (17) rad/s angular speed motor
Nm  = ww * igb/(2*pi);                      % (18) rps
N   = 60 * Nm;                              % (19) rpm


JT = m * r*r * (1 / (igb^2*ngb));         % (13)(15)moment of inertia
Tam = JT * Dwm;                               % (11)


Tm = (Trm + Tam);                           % (8)
Pmm = wm.*Tm;                              % (18) % Mechanical motor power


Fla = m*dv;                               % Vehicle mass acceleration
Pmw = (Ftr+Fla).*v;                        %


%%
figure (1) % V / T / P separated ECE IMPOSED
    subplot(3,1,1)
    ax=plot(v);
    ylabel(' Speed (m/s)')
    xlabel(' Time  (s)')
    grid on

    subplot(3,1,2)
    bx=plot(Tm)
    ylabel(' Torque (Nm)')
    xlabel(' Time  (s)')
    grid on

    subplot(3,1,3)
    cx=plot(Pmm)
    ylabel(' Power (W)')
    xlabel(' Time  (s)')
    grid on;
```

```
% figure (2) % V / T / P Together Only to see
% Pmk=Pmm/1000;
%     dy= plot(Pmk,'b');
%     hold on;
%     ey= plot(Tm,'r');
%     fy= plot(v,'m');
%     ylabel(' Tm(Nm) v(m/s) Pmm(kW)')
%     xlabel(' Time (s)')

figure (3) % Distribution Torque
    subplot(3,1,1)
    ay=plot(Tm);
    grid on;
    ylabel(' Tm (Nm)')
    xlabel(' Time  (s)')

    subplot(3,1,2)
    by=plot(Trm);
    grid on;
    ylabel(' Trm (Nm)')
    xlabel(' Time  (s)')
    title('Trm');

    subplot(3,1,3)
    cy=plot(Tam);
    grid on;
    ylabel(' Tam (Nm)')
    xlabel(' Time  (s)')
    title('Ta');

figure (4) % rpm wheels and rpm motor
   subplot(2,1,1)
   gy= plot(v,'b');
   ylabel(' v (m/s)')
   xlabel(' Time  (s)')
   grid on;

   subplot(2,1,2)
   hy= plot(N,'r');
   ylabel(' Motor speed (rpm)')
   xlabel(' Time  (s)')
   grid on;



figure (5) %Pmm / Pmw

   jy= plot(Pmm,'b');
   hold on; grid on;
   ky= plot(Pmw,'r');
   ylabel('Power (W)')
   xlabel(' Time (s)')

figure (6) % ECE 15
    subplot(2,1,1)
    my=plot(v, 'b');
    ylabel(' Speed (m/s)')
    xlabel(' Time  (s)')
    grid on;

    subplot(2,1,2)
    by=plot(dv, 'r')
    ylabel(' Acceleration (m/s^2)')
    xlabel(' Time  (s)')
    grid on;
```

## A.2.- Battery technical data


## Model: SP-LFP40AHA

| Item | | specification | Remark |
|---|---|---|---|
| Product Model | | SP-LFP40AHA | |
| Nominal Capacity | | 40Ah | |
| Nominal Voltage | | 3.2V | |
| Weight | | 1.5±0.1Kg | |
| Internal Impedance | | ≤0.8mΩ | AC1kHz |
| Cycle Life | | ≥2000Times | 80%DOD |
| Self-discharge rate | | ≤5% | 25℃, 1 month |
| Dimensions | Height | 186±1mm | |
| | Width | 116±1mm | |
| | Thickness | 46±0.5mm | |
| Charge | Standard Current | 13A | CC&CV |
| | Max. Current | 80A | 2C |
| | Limited Voltage | 3.65V | |
| | Cut-off Current | 0.8A | 0.02C |
| Discharge | Standard Current | 13A | |
| | Max. Current | 120A | 3C |
| | Cut-off Voltage | 2.5V | |
| Operation Temperature | Charge | 0℃～45℃ | |
| | Discharge | -20℃～55℃ | |
| Storage Temperature | | -10℃~45℃ | |
| Storage Humidity | | 25%~85% | RH |

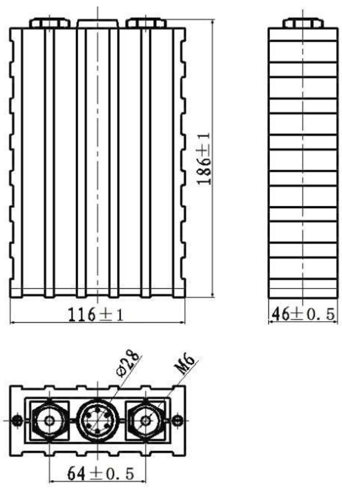

# SP-LFP40AHA cell specification

| | | |
|---|---|---|
| Model name | SP-LFP40AHA | |
| Nominal voltage | 3.2 V | Operating voltage under load is 3.0 V |
| Capacity | 40 AH | +/- 5% |
| Internal impenetrableness | ≤ 0.8mΩ | AC1kHz |
| Operating voltage | min 2.8V - max 3,65 V | At 80% DOD |
| Discharging cut-off voltage | 2.65 V | The cells is damaged if voltage drops below this level |
| Charging cut-off voltage | 3.7 V | The cells is damaged if voltage exceeds this level |
| Recommended charging - discharging Current | 13 A | 0.3 C |
| Maximum charging current | 80 A | 2 C |
| Maximum discharging current | 120 A | 3 C |
| Life cycles | ≥ 2000Times | 0.3C, 80% DOD |
| Operating thermal ambient - charging | 0°C ~ 45°C | The battery temperature should not increase this level |
| Operating thermal ambient - discharging | -20°C ~ 55°C | The battery temperature should not increase this level |
| Storage thermal Ambient | -10°C ~ 45°C | The battery temperature should not increase this level |
| Shell Material | Plastic | flame retardants |
| Dimensions | 186 x 46 x 116 mm | Millimeters (tolerance +/- 1 mm) |
| Weight | 1,5 kg | Kilograms (tolerance +/- 100g) |

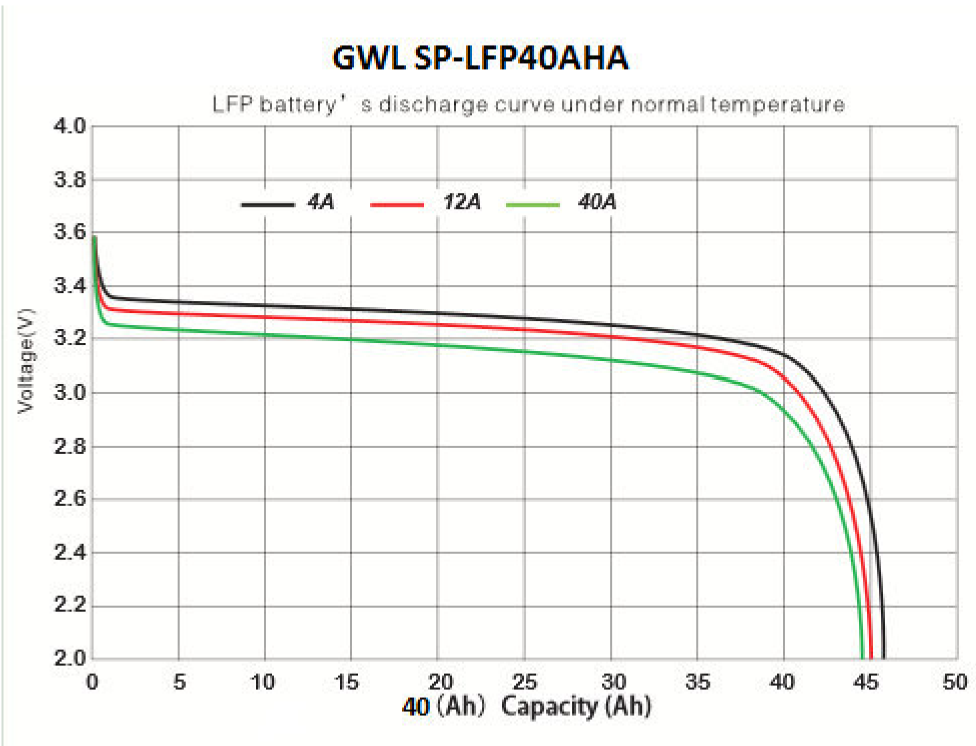

## A.3.- Charger Specification

**POW72V35A/BMS CHARGER SPECIFICATION**

| 1. Input characteristics | | | | |
|---|---|---|---|---|
| **No.** | **Item** | **Technical specification** | **Unit** | **Remark** |
| 1-1 | Rated input voltage | 230V | Vac | |
| 1-2 | Input voltage range | 180V – 264V | Vac | |
| 1-3 | AC input voltage frequency | 47 - 63 | Hz | |
| 1-4 | Inrush current | < 100 A | A | @ 264Vac start-up in cold condition |
| 1-5 | Max input current | 16 A | A | |

| 2. Output characteristics | | | | |
|---|---|---|---|---|
| **No.** | **Item** | **Technical specification** | **Unit** | **Remark** |
| 2-1 | Nominal charge voltage | 72V | Vdc | 24 cells @ 3.00V<br>6 batteries @ 12.00V |
| 2-2 | Fast charge voltage (V-max) | 88V | Vdc | 24 cells @ 4.00V<br>6 batteries @ 16.00V |
| 2-3 | Maintain voltage | 88V | Vac | (Float voltage, same as V-MAX) |
| 2-4 | Constant current (I-CC) | 35A | A | Maximal current during full charge |
| 2-5 | Deep voltage level (V-deep) | 65V | Vac | Deep discharge voltage level, bellow this voltage, the current is limited to I-min |
| 2-6 | Deep discharge current (I-min) | 8A | A | The limited current bellow V-Deep |
| 2-7 | BMS limit current (I-BMS) | 3A | A | The limited current for cell balancing (controlled by BMS) |
| 2-8 | Power efficiency | >80% | | @ 230Vac |

| 3. Protection characteristics | | | | |
|---|---|---|---|---|
| **No.** | **Item** | **Technical specification** | **Unit** | **Remark** |
| 3-1 | Output over voltage protection | 104 V | Vdc | |
| 3-2 | Software over voltage protection | The charger software limits the maximum output voltage to a level suitable for the connected battery system | | |
| 3-3 | Thermal cutback | The internal temperature monitor reduces the charger output power in extreme operational temperature to prevent damage | | |
| 3-4 | Output current limiting protection | 40 A | A | @ CC Mode |
| 3-5 | Output short circuit protection | Short circuit protection at the output terminals. Automatic recovery after restoring to normal conditions. | | |
| 3-6 | Electronic reverse battery protection | The charger is electronically protected against permanent reversed battery connection. | | |

| **4. Charge indicator (LED)** | | | | |
|---|---|---|---|---|
| **No.** | **Item** | **Technical specification** | **Unit** | **Remark** |
| 4-1 | Deep charging | LED flashing (slow) | | |
| 4-2 | Fast charging | LED flashing (fast) | | |
| 4-3 | Complete charge | LED on | | |
| 4-4 | Voltage indicator | LED display (00.00 to 99.99) | V | Not calibrated measuring, indication only |
| 4-5 | Current indicator | LED display (00.00 to 99.99) | A | |

| **5. Safety & EMC (CE Conformity Requirements)** | | | | |
|---|---|---|---|---|
| **No.** | **Item** | **Technical specification** | **Unit** | **Remark** |
| 5-1 | Electric strength test input – output | 1500 V / 10 mA /1 minute | Vac | No breakdown |
| 5-2 | Isolation resistance | > 10 MOhm @ 500 Vdc | MOhm | Input – ground (GND) |
| 5-3 | Isolation resistance | > 10 MOhm @ 500 Vdc | MOhm | Output – ground (GND) |
| 5-4 | Leakage current | < 3.5 mA | A | Vin = 264Vac, 50-60 Hz |
| 5-5 | Safety | EU standards for small electrical appliances | | CE MARK |
| 5-6 | EMC – RE | Class B | | EN55014 |
| 5-7 | EMC – CE | Class B | | EN55014 |
| 5-8 | EMC – air discharge | Level 3 | | EN61000-4-2 (dis. B) |
| 5-9 | EMC – contact discharge | Level 3 | | EN61000-4-2 (dis. B) |
| 5-10 | EMC – RS | Level 3 | | EN61000-4-6 (dis. A) |
| 5-11 | EMC – CS | Level 3 | | EN61000-4-3 (dis. A) |
| 5-10 | EMC – EFT | Level 3 | | EN61000-4-4 (dis. B) |
| 5-10 | EMC – Surge | Level 3 | | EN61000-4-5 (dis. A)<br>1 kV, 2 kV (dis. B) |

| **6. Environmental test requirements** | | | | |
|---|---|---|---|---|
| **No.** | **Item** | **Technical specification** | **Unit** | **Remark** |
| 6-1 | High ambient operating temperature | +40 °C | deg C | continuous operation |
| 6-2 | Low ambient operating temperature | -10 °C | deg C | continuous operation |
| 6-3 | Highest storage temperature | +70 °C | deg C | allow 2 hours to recover to normal temperature |
| 6-4 | Lowest storage temperature | -40 °C | deg C | allow 2 hours to recover to normal temperature |
| 6-5 | Drop shock | 40 g peak | | EN60068-2-32:1993 |

**7. Charging curve (current A – red, voltage V - blue)**

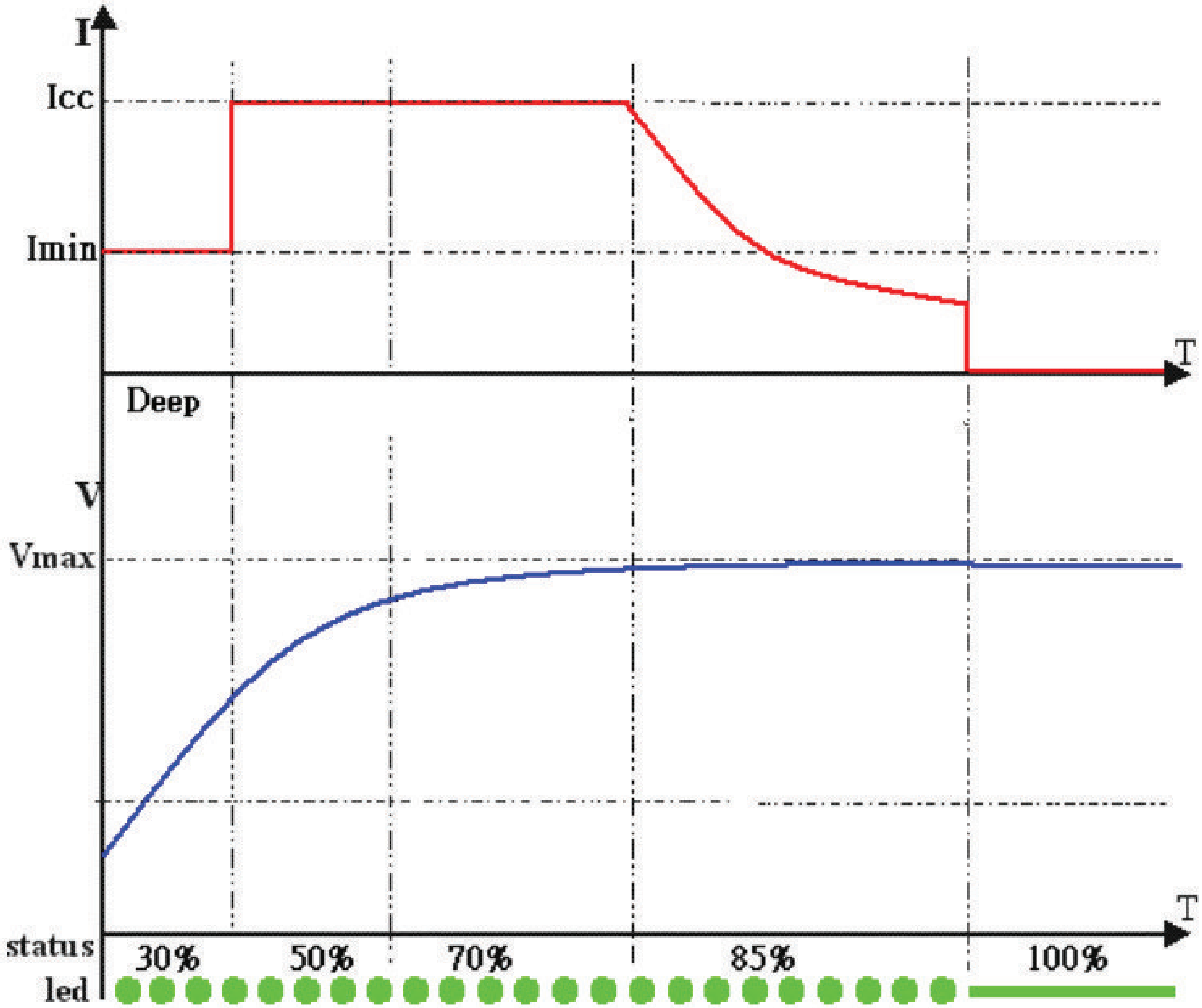

## 8. BMS connector operation

| Contacts | Status | Comment |
|---|---|---|
| VC12V | not connected | the charger works the standard way at MAX power |
| ON/OFF | not connected | |
| HIGH/LOW | not connected | |
| GND | not connected | |

| Contacts | Status | Comment |
|---|---|---|
| VC12V | +12V | the charger works the standard way at MAX power |
| ON/OFF | GND | |
| HIGH/LOW | GND | |
| GND | GND | |

| Contacts | Status | Comment |
|---|---|---|
| VC12V | +12V | the charger stops working |
| ON/OFF | not connected | |
| HIGH/LOW | any | |
| GND | GND | |

| Contacts | Status | Comment |
|---|---|---|
| VC12V | +12V | the charger works the standard way at REDUCED power (10%) |
| ON/OFF | GND | |
| HIGH/LOW | not connected | |
| GND | GND | |

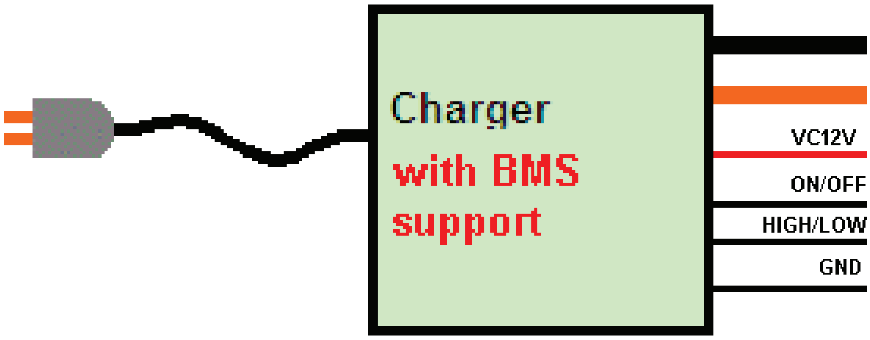

## A.4.- BMS123 Communication protocol

1. After sending a '$' ( 2400 Bd, 1 start- ,1 stop-bit, no parity ) the system will respond with a string, containing all the info ( and a bit more ) that is showed on the electronic dashboard.

These strings are continously sent, as long as '$'-signs are received regularly.

2. Each complete string shows 9 different fixed length 'measurements', and are sent like this :

0XXXXX 1XXXXX 0XXXXX 2XXXXX 0XXXXX 3XXXXX 0XXXXX 4XXXXX

0XXXXX 5XXXXX 0XXXXX 6XXXXX 0XXXXX 7XXXXX 0XXXXX 8XXXXX

The leading character indicates which data is sent. Each individual string of 6 Ascii-character is followed by an Ascii 'space', except measurement '4' and '8'...they are followed by an Ascii 'cr'.

'0' = sensor-type and current measurement
'1' = cell# with minimum voltage
'2' = cell# with maximum voltage
'3' = cell# with minimum temperature
'4' = cell# with maimum temperature
'5' = total system voltage
'6' = # charge level, voltmeter selected, capacity
'7' = 5 error indicators
'8' = real-time clock and charging-bit

remark: for reasons of "realtime feeling" during driving of the EV, we have decided to send the current-measurement more often then the other measurements.

3. Description of the structure of string '0'
-------------------------------------------------------------

After the '0', a character is sent ascii 31, 32 or 34 to indicate which current-sensor has been selected: 100, 200 or 400 Amp. Then an Ascii '+' or '-' sign is sent to indicate the polarity of the current measured.

Finally the measured current is sent, in the three remaining characters in hex-format. ( the minimum would thus be "-1FF", the maximum "+1FF" . In combination with the current-sensor used, the real current can be easily computed )

4. Description of the structure of string '1'
-------------------------------------------------------------

After the '1', two characters indicate in hex-format which cell has the lowest voltage. ( cell number ranges from '01' to 'FF' ) The next three characters indicate the cell voltage. Step-size is 0,005 Volt, so a cell- voltage of 3,3 Volt, would give a hex reading of '294'.

5. Description of the structure of string '2'
-------------------------------------------------------------

After the '2', two characters indicate in hex-format which cell has the highest voltage. (cell number ranges from '01' to 'FF') The next three characters indicate the cell voltage. Step-size is 0,005 Volt, so a cell-voltage of 3,3 Volt, would give a hex reading of '294'.

6. Description of the structure of string '3'
-------------------------------------------------------------

After the '3', two characters indicate in hex-format which cell has the lowest temperature. ( cell number ranges from '01' to 'FF' )The next three characters indicate the cell temperature. Step-size is 1,0 degree, and a cell temperature of zero degrees Centigrade would produce a reading of hex '113'. The decimal range is minus 40 to plus 99 degrees Celsius.

## 7. Description of the structure of string '4'

After the '4', two characters indicate in hex-format which cell has the highest temperature. ( cell number ranges from '01' to 'FF' ). The next three characters indicate the cell temperature. Step-size is 1,0 degree, and cell temperature of zero degrees Centigrade would produce a reading of hex '113'. The decimal range is minus 40 to plus 99 degrees Celsius.

## 8. Description of the structure of string '5'

After the '5', five characters indicate (in hex-format) the total system voltage. Step-size is 0,005 Volt, so a system-voltage of 100 Volts, would give a hex reading of '04E20'.

## 9. Description of the structure of string '6'

After the '6', 2 characters indicate (in hex format) the actual charge level in the string (HEX 0 to FF), the 1 character indicates the voltmeter-scale selected ( Ascii '0' to '4' ) and the remaining two charaaters indicate the remaining energy as a percentage 0 to 100 percent ; in hex-format this would translate in 0 to 64 %.

## 10. Description of the structure of string '7'

After the '7', 5 characters indicate the five error-indicators on the dashboard

#1 '1' of '0' --> Error-lamp
#2 '1' of '0' --> H-lamp ( high temp or voltage margin exceeded )
#3 '1' of '0' --> L-lamp ( low temp or voltage margin exceeded )
#4 '1' of '0' --> Mains lamp ( meaning mains is connected )
#5 '1' --> quick-charge selected '0' --> quick-charge active
'3' --> balanced charge selected, '2' --> balanced-charge active

## 11. Description of the structure of string '8'

After the '8', 4 characters indicate the real-time-clock in a BCD-fashion. So half-past twelve would read : '1230'
The remaining 5-th character indicates the charging-bit. So '0' means : charging is not allowed, '1' means : charging is allowed.

http://www.ev-power.eu

**EV-Power.eu** managed by **i4wifi a.s.** (member of GWL/Power group)
Prumyslova 11, CZ-10219 Prague 10, CZECH REPUBLIC (EU)
phone: +420 277 007 500, fax: +420 277 007 529, email: export@i4wifi.cz

GWL POWER

## A.5.- Electric Motor Catalogue

HEINZMANN®
Energy requires Control

PERM
TECHNOLOGY

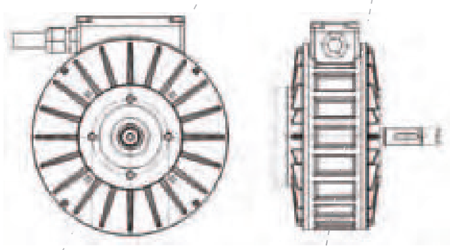

# PRODUCT CATALOGUE
## Disc Motors




# PMS 120

PERM TECHNOLOGY

(SL-EC 160, Type 22B)

Weight: approx. 12.3 kg
Inertia: 26.3 kg · cm²

| | | Output power | Speed | Torque | Current | Stall torque | Stall current | Max. stall torque | Max. stall current | Back-EMF constant | Torque constant |
|---|---|---|---|---|---|---|---|---|---|---|---|
| | | P | n | M | I | $M_o$ | $I_o$ | $M_{omax}$ | $I_{omax}$ | $K_e$ | $K_t$ |
| | | kW | $min^{-1}$ | Nm | A | Nm | A | Nm | A | $V/1000min^{-1}$ | Nm/A |
| **48 VDC** | *Self cooling* | 2,4 | 1500 | 15,3 | 58,8 | 18,3 | 70,6 | 40 | 155 | 17,7 | 0,26 |
| | | 3,5 | 3000 | 11,1 | 83,7 | 13,3 | 100,4 | 40 | 300 | 8,8 | 0,13 |
| | | 4,2 | 4500 | 8,9 | 96,9 | 10,7 | 116,3 | 40 | 440 | 6,0 | 0,09 |
| | *External ventilation* | 3,0 | 1500 | 19,1 | 74,9 | 22,9 | 89,9 | 41 | 160 | 17,7 | 0,26 |
| | | 5,3 | 3000 | 16,9 | 126,9 | 20,3 | 152,3 | 41 | 310 | 8,8 | 0,13 |
| | | 6,3 | 4500 | 13,3 | 146,2 | 16,0 | 175,4 | 40 | 440 | 6,0 | 0,09 |
| | | 6,3 | 6000 | 10,0 | 146,5 | 12,0 | 175,8 | 40 | 580 | 4,3 | 0,07 |
| **80 VDC** | *Self cooling* | 2,5 | 1500 | 15,9 | 35,9 | 19,1 | 43,1 | 40 | 90 | 29,7 | 0,44 |
| | | 4,4 | 3000 | 14,0 | 62,6 | 16,8 | 75,1 | 40 | 180 | 14,9 | 0,22 |
| | | 4,3 | 4500 | 9,1 | 59,0 | 11,0 | 70,8 | 40 | 260 | 10,2 | 0,15 |
| | *External ventilation* | 3,0 | 1500 | 19,1 | 44,4 | 22,9 | 53,3 | 45 | 105 | 29,7 | 0,43 |
| | | 5,8 | 3000 | 18,5 | 82,4 | 22,2 | 98,9 | 45 | 200 | 14,8 | 0,22 |
| | | 7,0 | 4500 | 14,9 | 98,5 | 17,8 | 118,2 | 45 | 300 | 10,2 | 0,15 |
| | | 7,5 | 6000 | 11,9 | 108,9 | 14,3 | 130,7 | 40 | 370 | 7,5 | 0,11 |
| | *Liquid cooling* | 3,7 | 1500 | 23,5 | 54,7 | 28,2 | 65,6 | 45 | 105 | 29,7 | 0,43 |
| | | 7,5 | 3000 | 23,9 | 107,1 | 28,7 | 128,5 | 45 | 200 | 14,8 | 0,22 |
| | | 9,5 | 4500 | 20,2 | 131,0 | 24,2 | 157,2 | 45 | 290 | 10,2 | 0,15 |
| | | 10,0 | 6000 | 15,9 | 144,5 | 19,1 | 173,4 | 40 | 360 | 7,5 | 0,11 |
| **96 VDC** | *Self cooling* | 2,4 | 1500 | 15,3 | 30,2 | 18,4 | 36,2 | 40 | 80 | 34,8 | 0,51 |
| | | 3,8 | 3000 | 12,1 | 43,9 | 14,5 | 52,7 | 40 | 150 | 18,1 | 0,28 |
| | | 4,0 | 4500 | 8,5 | 49,1 | 10,2 | 58,9 | 40 | 230 | 11,6 | 0,17 |
| | *External ventilation* | 3,0 | 1500 | 19,1 | 38,7 | 22,9 | 46,4 | 45 | 92 | 34,8 | 0,49 |
| | | 5,3 | 3000 | 16,9 | 61,4 | 20,3 | 73,7 | 45 | 165 | 18,1 | 0,27 |
| | | 7,0 | 4500 | 14,9 | 87,2 | 17,8 | 104,6 | 45 | 270 | 11,6 | 0,17 |
| | | 7,5 | 6000 | 11,9 | 95,3 | 14,3 | 114,4 | 40 | 320 | 8,5 | 0,13 |
| | *Liquid cooling* | 3,7 | 1500 | 23,6 | 47,7 | 28,3 | 57,2 | 45 | 91 | 34,3 | 0,49 |
| | | 7,5 | 3000 | 23,9 | 96,4 | 28,7 | 115,7 | 45 | 180 | 16,7 | 0,25 |
| | | 10,5 | 4500 | 22,3 | 127,4 | 26,7 | 152,9 | 45 | 260 | 11,6 | 0,17 |
| | | 11,0 | 6000 | 17,5 | 137,3 | 21,0 | 164,8 | 40 | 310 | 8,6 | 0,13 |
| **330 VDC** | *Self cooling* | 2,2 | 1500 | 14,0 | 10,3 | 16,8 | 12,4 | 41 | 30 | 89,9 | 1,35 |
| | | 4,2 | 3000 | 13,3 | 18,5 | 16,0 | 22,2 | 40 | 55 | 48,1 | 0,72 |
| | | 4,0 | 4500 | 8,5 | 16,7 | 10,2 | 20,0 | 40 | 80 | 33,8 | 0,51 |
| | *External ventilation* | 2,8 | 1500 | 17,8 | 13,4 | 21,4 | 16,1 | 45 | 33 | 89,9 | 1,33 |
| | | 5,8 | 3000 | 18,5 | 25,6 | 22,2 | 30,7 | 45 | 61 | 48,2 | 0,72 |
| | | 7,0 | 4500 | 14,8 | 29,4 | 17,8 | 35,3 | 45 | 87 | 33,7 | 0,51 |
| | | 7,0 | 6000 | 11,1 | 30,6 | 13,3 | 36,7 | 40 | 110 | 24,9 | 0,36 |
| | *Liquid cooling* | 3,8 | 1500 | 24,2 | 15,5 | 29,0 | 18,6 | 45 | 30 | 105,9 | 1,56 |
| | | 7,5 | 3000 | 23,9 | 33,0 | 28,7 | 39,6 | 45 | 62 | 48,2 | 0,72 |
| | | 10,5 | 4500 | 22,3 | 41,9 | 26,7 | 50,3 | 45 | 85 | 35,3 | 0,53 |
| | | 11,0 | 6000 | 17,5 | 47,7 | 21,0 | 57,2 | 40 | 110 | 24,9 | 0,37 |
| **560 VDC** | *Self cooling* | 2,2 | 1500 | 14,0 | 4,4 | 16,8 | 5,3 | 41 | 13 | 205,6 | 3,17 |
| | | 4,2 | 3000 | 13,3 | 8,4 | 16,0 | 10,1 | 40 | 25 | 103,5 | 1,59 |
| | | 4,0 | 4500 | 8,5 | 8,7 | 10,2 | 10,4 | 40 | 42 | 64,3 | 0,97 |
| | *External ventilation* | 2,8 | 1500 | 17,8 | 5,7 | 21,4 | 6,8 | 44 | 14 | 205,6 | 3,12 |
| | | 5,8 | 3000 | 18,5 | 11,3 | 22,1 | 13,6 | 44 | 27 | 103,5 | 1,63 |
| | | 7,0 | 4500 | 14,8 | 15,4 | 17,8 | 18,5 | 44 | 46 | 64,3 | 0,96 |
| | | 7,3 | 6000 | 11,6 | 16,2 | 13,9 | 19,4 | 41 | 57 | 48,7 | 0,72 |
| | *Liquid cooling* | 3,8 | 1500 | 24,2 | 7,8 | 29,0 | 9,4 | 45 | 15 | 205,6 | 3,12 |
| | | 7,5 | 3000 | 23,9 | 15,5 | 28,7 | 18,6 | 45 | 29 | 103,5 | 1,54 |
| | | 11,0 | 4500 | 23,3 | 24,1 | 28,0 | 28,9 | 45 | 47 | 64,3 | 0,97 |
| | | 11,5 | 6000 | 18,3 | 25,3 | 22,0 | 30,4 | 40 | 62 | 48,8 | 0,72 |

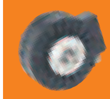

## A.6.- SEV CON technical data

Partner with Performance


# Gen4

## AC MOTOR CONTROLLER

The Gen4 range represents the latest design in compact AC Controllers. These reliable controllers are intended for on-road and off-road electric vehicles and feature the smallest size in the industry for their power capacity.

Thanks to the high efficiency it is possible to integrate these controllers into very tight spaces without sacrificing performance. The design has been optimised for the lowest possible installed cost while maintaining superior reliability in the most demanding applications.

## FEATURES

- Advance flux vector control
- Autocheck system diagnostic
- Integrated logic circuit
- Hardware & software failsafe watchdog operation
- Supports both PMAC motor and AC induction motor control
- Integrated fuse holder
- IP66 protection

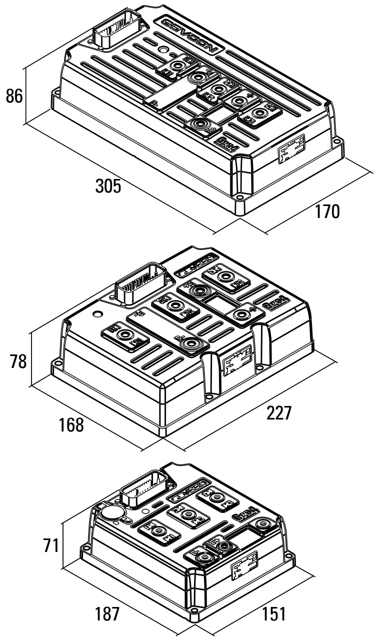


# Gen4

## KEY PARAMETERS

| Model | Size 2 | Size 4 | Size 6 | Size 2 | Size 4 | Size 6 | Size 2 | Size 4 | Size 6 | Size 2* | Size 4 | Size 6* |
|---|---|---|---|---|---|---|---|---|---|---|---|---|
| Nominal Battery Voltage | 24 VDC | 24 to 36 VDC | | 36 to 48 VDC | | | 72 to 80 VDC | | | 96 to 120 VDC | | |
| Max operating voltage | 34.8 VDC | 52.2 VDC | | 69.6 VDC | | | 116 VDC | | | 150 VDC | | |
| Min. operating voltage | 12.7 VDC | | | 19.3 VDC | | | 39.1 VDC | | | 48 VDC | | |
| Peak Current (2min) | 300A | 450A | 650A | 275A | 450A | 650A | 180A | 350A | 550A | 150A | 300A | 450A |
| Boost Current (10 sec) | 360A | 540A | 780A | 330A | 540A | 780A | 215A | 420A | 660A | 180A | 360A | 540A |
| Cont. Current (60 min) | 120A | 180A | 260A | 110A | 180A | 260A | 75A | 140A | 220A | 60A | 120A | 180A |

*Not yet available. Please contact Sevcon.

## MULTIPLE MOTOR FEEDBACK OPTIONS

Gen4 provides a number of motor feedback possibilities from a range of hardware inputs and software control, allowing a great deal of flexibility.

- Absolute UVW encoder input
- Absolute Sin/Cos encoder input
- Incremental AB encoder input

## INTEGRATED I/O

Gen4 includes a fully-integrated set of inputs and outputs (I/O) designed to handle a wide range of vehicle requirements.  This eliminated the need for additional external I/O modules or vehicle controllers and connectors.

- 8 digital inputs
- 2 analogue inputs (can be configured as digital)
- 3 contactor/solenoid outputs
- 1 encoder supply output - programmable 5V or 10V

## OTHER FEATURES

- A CANopen bus allows easy interconnection of controllers and devices such as displays and driver controls.
- The CANbus allows the user to wire the vehicle to best suit vehicle layout since inputs and outputs can be connected to any of the controllers on the vehicle and the desired status is passed over the CAN network to the relevant motor controller.
- The Gen4 controller can dynamically change the allowed battery current by exchanging CAN messages with a compatible Battery Management System.
- Configurable as vehicle control master or motor slave.

## CONFIGURATION TOOLS

Sevcon offers a range of configuration tools for the Gen4 controller, with options for Windows based PC or calibrator  handset unit. These tools provide a simple yet powerful means  of accessing the CANopen bus for diagnostics or parameter adjustment. The handset unit features password protected access levels and a customized logo start-up screen.

SEVCON®

Partner with Performance

Sevcon Ltd Kingsway South
Gateshead NE11 0QA England
T +44 (0191) 497 9000
sales.uk@sevcon.com

Sevcon Inc 155 Northboro Road
Southborough MA01772 USA
T +1 (508) 281 5500
sales.us@sevcon.com

Sevcon SAS Parc d'Activité
du Vert Galant Rue Saint Simon
St Ouen l'Aumône
95041 Cergy Pontoise Cedex France
T +33 (0)1 34 30 35 00
sales.fr@sevcon.com

Sevcon Japan K.K.
Kansai Office 51-26 Ohyabu Hikone
Shiga Japan 522-0053
T +81 (0) 7 49465766
jp.info@sevcon.com

Sevcon Asia Ltd
Room No.202 Dong-Ah Heights Bldg
449-1 Sang-Dong Wonmi-Gu
Bucheon City Gyeounggi-Do
420-816 Korea
T +82 32 215 5070
sales.kr@sevcon.com

Sevcon Germany
Hintere Str.32
73266 Bissingen an der Teck
Germany
T: +49 (0)170 9980294
E: de.info@sevcon.com

follow @Sevcon
www.sevcon.com

## A.7.- SEW technical data

SEW EURODRIVE

# MOVIDRIVE® MDX60B/61B

Edition

02/2004

## Operating Instructions

1122 2913 / EN

### *Size 3 (400/500 V units)*

| MOVIDRIVE® MDX61B | | 0150-503-4-0_ | 0220-503-4-0_ | 0300-503-4-0_ |
|---|---|---|---|---|
| **INPUT** | | | | |
| Supply voltage | $V_{mains}$ | 3 × AC 380 V –10 % ... 3 × AC 500 V +10 % | | |
| Supply frequency | $f_{mains}$ | 50 Hz ... 60 Hz ±5 % | | |
| Rated mains current[1)] (at $V_{mains}$ = 3 × AC 400 V) | 100 % $I_{mains}$<br>125 % | AC 28.8 A<br>AC 36.0 A | AC 41.4 A<br>AC 51.7 A | AC 54.0 A<br>AC 67.5 A |
| **OUTPUT** | | | | |
| Rated output power[2)] (at $V_{mains}$ = 3 × AC 400 V...AC 500 V) | $P_N$ | 22.2 kVA | 31.9 kVA | 41.6 kVA |
| Rated output current[1)] (at $V_{mains}$ = 3 × AC 400 V) | $I_N$ | AC 32 A | AC 46 A | AC 60 A |
| Current limitation | $I_{max}$ | Motor and regenerative 150 % $I_N$, duration depending on the capacity utilization | | |
| Internal current limitation | | $I_{max}$ = 0...150 % can be set in menu (P303 / P313) | | |
| Minimum permitted brake resistance value (4Q operation) | $R_{BRmin}$ | 15 Ω | | 12 Ω |
| Output voltage | $V_{out}$ | max. $V_{mains}$ | | |
| PWM frequency | $f_{PWM}$ | Adjustable: 4/8/16 kHz (P860 / P861 / P864) | | |
| Speed range / resolution | $n_A$ / $\Delta n_A$ | -6000 ... 0 ... +6000 $min^{-1}$ / 0.2 $min^{-1}$ across the entire range | | |
| **GENERAL** | | | | |
| Power loss at $P_N$ | $P_{Vmax}$ | 550 W | 750 W | 950 W |
| Cooling air consumption | | 180 $m^3$/h (108 $ft^3$/min) | | |
| Weight | | 15.0 kg (33.07 lb) | | |
| Dimensions | W × H × D | 200 × 465 × 308 mm (7.87 × 18.31× 12.13 in) | | |

1) The rated mains currents and output currents must be 20 % below the rated data at $V_{mains}$ = 3 × AC 500 V.

2) The performance data apply to $f_{PWM}$ = 4 kHz (factory setting in VFC operating modes).

| MDX61B Standard version | 0150-503-4-00 | 0220-503-4-00 | 0300-503-4-00 |
|---|---|---|---|
| Part number | 827 964 0 | 827 965 9 | 827 966 7 |
| **MDX61B Application version** | **0150-503-4-0T** | **0220-503-4-0T** | **0300-503-4-0T** |
| Part number | 827 982 9 | 827 983 7 | 827 984 5 |
| Constant load<br>Recommended motor power $P_{mot}$ | 15 kW (20 HP) | 22 kW (30 HP) | 30 kW (40 HP) |
| Variable torque load or constant load without overload<br>Recommended motor power $P_{mot}$ | 22 kW (30 HP) | 30 kW (40 HP) | 37 kW (50 HP) |
| VFC operating mode ($f_{PWM}$ = 4 kHz)<br>Continuous output current = 125 % $I_N$ $I_D$<br>(at $V_{mains}$ = 3 × AC 400 V) | AC 40.0 A | AC 57.5 A | AC 75.0 A |
| CFC/SERVO operating mode ($f_{PWM}$ = 8 kHz)<br>Continuous output current = 100% $I_N$ $I_D$ | AC 32 A | AC 46 A | AC 60 A |

## A.8.- dSPACE technical data

www.dspace.com


# MicroAutoBox II

- dSPACE's robust and compact stand-alone prototyping unit
- Available with all major automotive bus systems, programmable FPGA, and Embedded PC
- Universal development system for the automotive field and many other applications (e.g., industrial, aerospace, medical engineering)
- NEW: Variants 1401/1511/1514 and 1401/1513/1514 with integrated Xilinx® Kintex®-7 FPGA for even more FPGA functionality

Embedded Success dSPACE

# Technical Details

| Parameter | | Specification | | | | |
|---|---|---|---|---|---|---|
| **MicroAutoBox II** | | **1401/1507** | **1401/1511** | **1401/1513** | **1401/1511/1514** | **1401/1513/1514** |
| Processor | | ■ IBM PPC 750GL, 900 MHz (incl. 1 MB level 2 cache) | | | | |
| Memory | | ■ 16 MB main memory<br>■ 6 MB memory exclusively for communication between MicroAutoBox and PC/notebook<br>■ 16 MB nonvolatile flash memory containing code section and flight recorder data<br>■ Clock/calendar function for time-stamping flight recorder data | | | | |
| Boot time | | ■ Depending on flash application size. Measurement examples: 1 MB application: 160 ms; 3 MB application: 340 ms | | | | |
| Inter-faces | Host interface | ■ 100/1000 Mbit/s Ethernet connection (TCP/IP). Fully compatible with standard network infrastructure. LEMO connector.<br>■ Optional XCP on Ethernet interface to support third-party calibration and measurement tools | | | | |
| | Ethernet real-time I/O interface | ■ 100/1000 Mbit/s Ethernet connection (UDP/IP; TCP/IP on request). RTI Ethernet (UDP) Blockset (optional) for read/write access. LEMO connector. | | | | |
| | USB interface | ■ USB 2.0 interface for long-term data acquisition with USB mass storage devices. LEMO connector. | | | | |
| | CAN interface | ■ 4 CAN channels | | ■ 6 CAN channels (partial networking supported) | ■ 4 CAN channels | ■ 6 CAN channels (partial networking supported) |
| | Serial interface (based on CAN processor) | ■ 2 x RS232 interface | | ■ 3 x RS232 interface | ■ 2 x RS232 interface | ■ 3 x RS232 interface |
| | | ■ 2 x serial interface usable as K/L-Line or LIN interface | | ■ 3 x serial interface usable as K/L-Line or LIN interface | ■ 2 x serial interface usable as K/L-Line or LIN interface | ■ 3 x serial interface usable as K/L-Line or LIN interface |
| | ECU interface | ■ 3 x dual-port memory interface | ■ 2 x dual-port memory interface | | | |
| | IP module slot for FlexRay and CAN FD | ■ 2 slots[1] for FlexRay[2] or CAN FD modules | – | – | ■ 2 slots[1] for FlexRay[2] or CAN FD modules | |
| Programmable FPGA | | – | – | – | ■ Xilinx® Kintex®-7 (XC7K325T) | |
| Analog input | Resolution | – | ■ 16 16-bit channels | ■ 32 16-bit channels | ■ 16 16-bit channels[3] | ■ 32 16-bit channels[3] |
| | Sampling | – | ■ 16 parallel channels with 1 Msps conversion rate | ■ 16 parallel channels with 1 Msps conversion rate<br>■ 16 multiplexed channels with 200 Ksps conversion rate | ■ 16 parallel channels with 1 Msps conversion rate | ■ 16 parallel channels with 1 Msps conversion rate<br>■ 16 multiplexed channels with 200 Ksps conversion rate |
| | Input voltage range | – | ■ 0 ... 5 V | ■ -10 ... 10 V | ■ 0 ... 5 V | ■ -10 ... 10 V |
| Analog output | Resolution | – | ■ 4 12-bit channels | ■ 8 16-bit channels | ■ 4 12-bit channels[3] | ■ 8 16-bit channels[3] |
| | Output voltage range | – | ■ 0 ... 4.5 V | ■ -10 ... 10 V | ■ 0 ... 4.5 V | ■ -10 ... 10 V |
| | Output current | – | ■ 5 mA max. | ■ 8 mA max. | ■ 5 mA max. | ■ 8 mA max. |
| Digital I/O | General | – [4] | ■ FPGA-based digital I/O<br>■ RTI software support for bit I/O, frequency, and PWM generation/measurements | | | |
| | Bit I/O | | ■ 40 inputs<br>■ 40 outputs, 5 mA output current | ■ 24 inputs<br>■ 24 outputs, 5 mA output current | ■ 40 inputs[3]<br>■ 40 outputs, 5 mA output current[3] | ■ 24 inputs[3]<br>■ 24 outputs, 5 mA output current[3] |
| | | | ■ Input / output logic levels: 5 V or levels up to 40 V (depending on $V_{Drive}$), selectable | | | |
| | PWM generation/ measurement | – | ■ All channels fully configurable as frequency or PWM inputs/outputs<br>■ PWM frequency 0.0003 Hz ... 150 KHz, duty cycle 0 ... 100%, up to 21-bit resolution | | | |
| Onboard sensors | | ■ Motion sensing with 3-axis accelerometer. Pressure sensing for altitude indication. | | | | |
| Signal conditioning | | ■ Signal conditioning for automotive signal levels, no power driver included<br>■ Overvoltage protection; overcurrent and short circuit protection | | | | |
| Physical connections | | ■ LEMO connectors for 2 ECU interfaces, Ethernet I/O interface, USB interface, and Ethernet host interface | | | | |
| | | ■ Ethernet host interface (100/1000 Mbit/s, TCP/IP) for notebook/PC connection (for program load, experiment configuration, signal monitoring, and flight recorder read-out) | | | | |
| | | ■ Integrated Ethernet switch | | | | |
| | | ■ Additional 78-pin Sub-D connector | ■ ZIF connector for I/O signals, mechanically secured, Sub-D connector for power supply | | | |

1) *IP module slot. Can also be used for other IP modules such as an ARINC interface module (via dSPACE Engineering Services).*
2) *i.e., 4 FlexRay channels, combination with CAN FD possible.*
3) *Additional channels with DS1552 (p. 12).*
4) *Additional digital I/O channels available via I/O extension on IP module slot (5 inputs and 2 outputs, or 2 inputs and 5 outputs, software-selectable, 5 V output level, 24 mA output current).*

| Parameter | | Specification | | | | |
|---|---|---|---|---|---|---|
| MicroAutoBox II | | 1401/1507 | 1401/1511 | 1401/1513 | 1401/1511/1514 | 1401/1513/1514 |
| Physical characteristics | Enclosure material | ■ Cast aluminum box | | | | |
| | Enclosure size | ■ Approx. 200 x 225 x 50 mm (7.9 x 8.9 x 2.0 in) | | | ■ Approx. 200 x 225 x 95 mm (7.9 x 8.9 x 3.8 in) | |
| | Temperature | ■ Operating (case) temperature: -40 ... +85 °C (-40 ... +185 °F)<br>■ Storage temperature: -55 ... +125 °C (-67 ... +257 °F) | | | | |
| | Power supply | ■ 6 ... 40 V input power supply, protected against overvoltage and reverse polarity | | | | |
| | Power consumption | ■ Max. 25 W | | | ■ Max. 50 W | |

## Order Information

| Products | Order Number |
|---|---|
| MicroAutoBox II 1401/1507 | ■ MABX_II_1507 |
| MicroAutoBox II 1401/1511 | ■ MABX_II_1511 |
| MicroAutoBox II 1401/1513 | ■ MABX_II_1513 |
| MicroAutoBox II 1401/1511/1514 | ■ MABX_II_1511/14 |
| MicroAutoBox II 1401/1513/1514 | ■ MABX_II_1513/14 |

## Relevant Software and Hardware

| Software | | Order Number |
|---|---|---|
| Included | ■ Data retrieval utility for flight recorder read-out | – |
| | ■ Comprehensive C libraries (e.g., digital I/O support) | – |
| Required | ■ Real-Time Interface (RTI) | ■ RTI |
| | ■ Microtec PowerPC C Compiler | ■ CCPPPC |
| Optional | ■ ControlDesk® Next Generation | Please see the relevant product information. |
| | ■ RTI CAN Blockset | ■ RTICAN_BS |
| | ■ RTI CAN MultiMessage Blockset | ■ RTICANMM_BS |
| | ■ RTI LIN MultiMessage Blockset | ■ RTILINMM_BS |
| | ■ dSPACE FlexRay Configuration Package | ■ FCP |
| | ■ RTI Bypass Blockset | ■ RTIBYPASS_BS |
| | ■ RTI AUTOSAR Blockset | Please see the relevant product information. |
| | ■ RTI Ethernet (UDP) Blockset | ■ RTI_ETH/UDP_BS |
| | ■ RTI USB Flight Recorder Blockset | ■ RTI_USB_FR_BS |
| | ■ AutomationDesk | ■ AUD |
| | ■ RTI FPGA Programming Blockset[1] | Please see the relevant product information. |
| | ■ RTI DS1552 I/O Extension Blockset (p. 12) | ■ RTI1552_I/O_EXT_ BS |
| | ■ MABXII Cylinder Pressure Indication Solution (p. 12) | ■ MABXII_CPI_CPU |
| | ■ MicroAutoBox II AC Motor Control Solution Blockset | ■ MABXII_ACMC_BS |
| | ■ RTI Watchdog Blockset (p. 8) | ■ RTI_WATCHDOG_BS |
| | ■ XSG AC Motor Control Library | ■ FPGA_XSG_ACMC |
| | ■ XSG Utils Library | ■ FPGA_XSG_UTILS |
| | ■ NEW: XSG Advanced Engine Control Library (p. 13) | ■ FPGA_XSG_ENGCON |
| | ■ NEW: V2X Solution | ■ V2X_SOL |

[1] *Using the RTI FPGA Programming Blockset requires additional software, i.a. Xilinx® products, please see the relevant product information.*

| Hardware | | Order Number |
|---|---|---|
| Included | One Ethernet Interface Cable (ETH_CAB1) is already included with each purchased MicroAutoBox II. | – |
| Optional | ■ DS4340 FlexRay Interface Module (p. 16) | ■ DS4340 |
| | ■ DS4342 CAN FD Interface Module (p. 17) | ■ DS4342 |
| | ■ FlexRay interface cable for MicroAutoBox II 1401/1507 | ■ FR_CAB1 |
| | ■ FlexRay interface cable for MicroAutoBox II 1401/1511/1514 and 1401/1513/1514 | ■ FR_CAB3 |
| | ■ Ethernet interface cable (LEMO to RJ45 connector), 5 m | ■ ETH_CAB1 |
| | ■ Electrically isolated Ethernet interface cable (300 Vrms, LEMO to RJ45 connector) | ■ ETH_CAB2 |
| | ■ Ethernet cable to connect MicroAutoBox II and DCI-GSI2 | ■ ETH_CAB3 |
| | ■ Ethernet interface cable (LEMO to RJ45 connector), 10 m | ■ ETH_CAB4 |
| | ■ USB interface cable (LEMO to USB connector) for connection to mass storage devices ("flight recorder") | ■ USB_CAB13 |
| | ■ LVDS link cable to connect MicroAutoBox and DCI-GSI1 or DPMEM PODs (LEMO-1S to ZIF crimp contacts) | ■ LVDS_CAB1 |
| | ■ LVDS link cable LEMO-1S to LEMO-1S, 5 m, 85 °C | ■ LVDS_CAB15 |
| | ■ MicroAutoBox Break-Out Box (p. 20) | ■ DS1541 |
| | ■ DS1552 Multi-I/O Module (p. 12) | ■ DS1552 |
| | ■ DS1553 ACMC Module (p. 14) | ■ MABXII_ACMC |
| | ■ MicroAutoBox Embedded PC (p. 9) | ■ See p. 9 |
| | ■ Digital I/O extension for MABX II 1401/1507 | ■ MABXII_1507_DIO_SOL |
| | ■ MicroAutoBox II RapidPro Joining Plate (p. 8) | ■ RAPIDPRO_MABX_KIT |

## A.9.- USB – CAN Interface technical data

**Heinzmann GmbH & Co. KG**
**Engine & Turbine Management**
**Electric and Hybrid Drives**
D-79677 Schönau / Germany
www.heinzmann.com


# USB-to-CAN Interface

**USB-to-CAN compact - Intelligent low-cost CAN interface for the USB-Port**

The USB-to-CAN compact is a low-cost, active CAN interface for connection to the USB bus. The 16-bit microcontroller system enables reliable, loss-free transmission and reception of messages in CAN networks with both a high transmission rate and a high bus load. In addition, messages are provided with a time-stamp and can be filtered and buffered directly in the USB-to-CAN compact. The module can also be used as a master assembly, e.g. for CANopen systems. Together with the universal CAN driver VCI, supplied with the delivery, the USB-to-CAN compact allows the simple integration of PC-supported applications into CAN systems.

Combining an extremely attractive price with compact construction, the USB-to-CAN compact interface is ideal for use in series products and in conjunction with the canAnalyser for development, service and maintenance work.

**Technical Data**

| | |
|---|---|
| PC bus interface | USB, version 2.0 (full speed) |
| Microcontroller | Infineon C161U |
| CAN controller | SJA 1000 |
| CAN bus interface | ISO 11898-2, Sub D9 connector or RJ45 connector according to CiA 303-1 |
| Power supply | Provided by USB port, 250 mA typ |
| Galvanic isolation | optional (1 kV, 1 sec.) |
| Temperature range | -20 °C ... +80 °C |
| Certification | CE, FCC, CSA/UL, IEC 60950-1:2005 (2nd Edition) / EN 60950-1:2006 + A11:2009 |
| Size | 80 x 45 x 20 mm |

**Contents of delivery**
- USB CAN Interface
- User's manual
- CAN driver VCI for Windows 2000, XP, Vista, Windows 7
- Simple CAN monitor "miniMon"

## A.10.- ECE 15 driving cycle – data

Published Project Report
PPR354

Creating the future of transport

# A reference book of driving cycles for use in the measurement of road vehicle emissions

T J Barlow, S Latham, I S McCrae and P G Boulter

**Cycle No: 1**

| | |
|---|---|
| **Cycle name:** | **ECE 15** |
| **Alternative name:** | |
| **Test programme:** | **EU legislative cycles** |
| **Additional info:** | **Elementary ECE 15 cycle** |
| **Vehicle category:** | **Cars** |

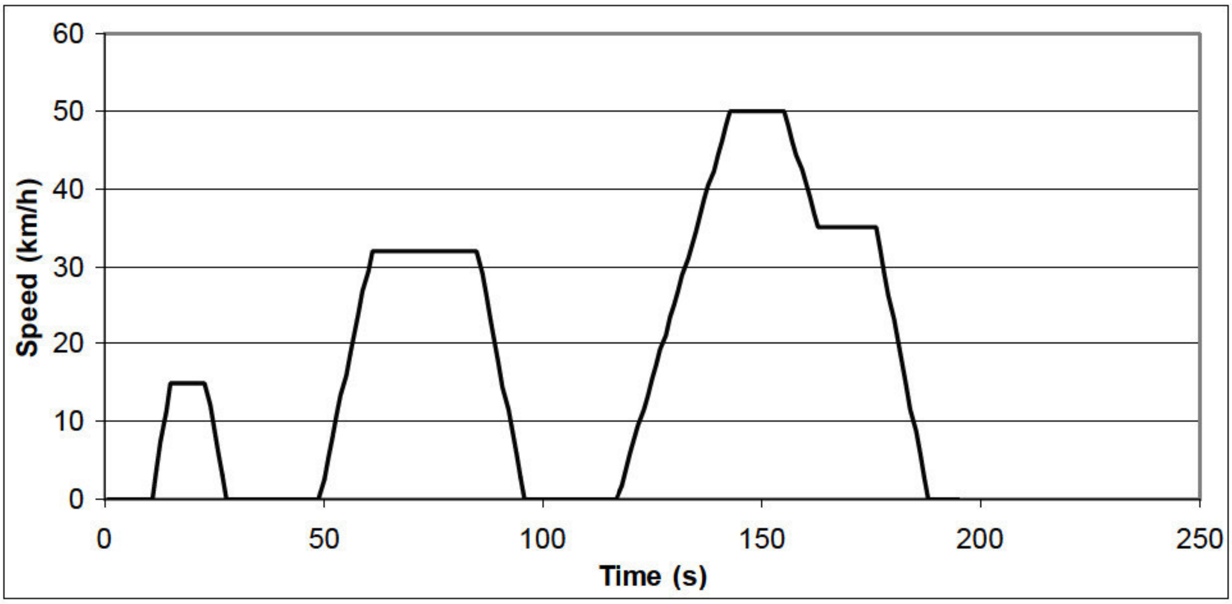


**ART.KINEMA parameters**

| | | | |
|---|---|---|---|
| Total distance | 994.6 m | Average negative acceleration | -0.393 $m/s^2$ |
| Total time | 195 s | Standard deviation of accel. | 0.473 $m/s^2$ |
| Driving time | 150 s | Standard dev. of positive accel. | 0.285 $m/s^2$ |
| Drive time | 49 s | Accel: 75th - 25th percentile | 0.254 $m/s^2$ |
| Drive time spent accelerating | 53 s | Number of accelerations | 3 |
| Drive time spent decelerating | 48 s | Accelerations per km | 3.016 /km |
| Time spent braking | 40 s | Number of stops | 4 |
| Standing time | 45 s | Stops per km | 4.02 /km |
| % of time driving | 76.92 % | Average stop duration | 11.25 s |
| % of cruising | 25.13 % | Average distance between stops | 248.65 m |
| % of time accelerating | 27.18 % | Relative positive acceleration | 0.147 $m/s^2$ |
| % of time decelerating | 24.62 % | Positive kinetic energy | 3.812 $m/s^2$ |
| % of time braking | 20.51 % | Relative positive speed | 0.521 |
| % of time standing | 23.08 % | Relative real speed | 0.763 |
| Average speed (trip) | 18.4 km/h | Relative square speed | 9.436 m/s |
| Average driving speed | 23.87 km/h | Relative positive square speed | 4.925 m/s |
| Standard deviation of speed | 15.58 km/h | Relative real square speed | 7.378 m/s |
| Speed: 75th - 25th percentile | 32.01 km/h | Relative cubic speed | 99.60 $m^2/s^2$ |
| Maximum speed | 50.07 km/h | Relative positive cubic speed | 52.09 $m^2/s^2$ |
| Average acceleration | 0.000 $m/s^2$ | Relative real cubic speed | 78.72 $m^2/s^2$ |
| Average positive acceleration | 0.348 $m/s^2$ | Root mean square of acceleration | 0.183 $m/s^2$ |